FCP Report No. 40

# FATIGUE OF LOW CARBON STEELS AS INFLUENCED BY REPEATED STRAIN AGING

by

Hüseyin Şehitoğlu
Department of Theoretical and Applied Mechanics

A "repeated strain aging" technique is introduced to enhance the yield strength of ASTM A-36 steel. Results obtained indicate that the yield strength may be increased as much as 55%. The fatigue behavior of repeatedly strained aged smooth specimens is examined. The same technique is applied to notched members to enhance the yield strength of the material at the notch root. Fatigue tests on repeatedly strain aged plates indicate that long life improvements are observed compared to unaged plates of the same material and geometry.

A Report of the
FRACTURE CONTROL PROGRAM
College of Engineering, University of Illinois
Urbana, Illinois 61801

June, 1981

## ACKNOWLEDGMENTS

This investigation was conducted in the Materials Engineering Research Laboratory, College of Engineering, Department of Theoretical and Applied Mechanics, University of Illinois, Urbana, with Professor R. T. Shield as Department Head. Financial support was provided by the Fracture Control Program, College of Engineering, University of Illinois.

Professor JoDean Morrow is gratefully acknowledged for his assistance, patience and many stimulating discussions throughout this research. Professor G. M. Sinclair made helpful suggestions in the course of this investigation. Acknowledgment also goes to Professor Darrell F. Socie, Mr. Peter Kurath, and Mr. Tom Deves for stimulating discussions. Messrs. Todd Christopherson, Eliot Zaiken, and Scott Birnbaum are thanked for assisting during the experiments. Mrs. Darlene Mathine is specially thanked for typing the manuscript.

## TABLE OF CONTENTS

LIST OF TABLES

## LIST OF FIGURES

# LIST OF SYMBOLS

<u>Note</u>: Quantity in parenthesis ( ) is the symbol used in computer plots.

| | |
|---|---|
| a (A) | Crack length measured from the notch root |
| b | Fatigue strength exponent (Basquin's exponent) |
| c | Fatigue ductility exponent (Coffin's exponent) |
| C | $\sigma_a/\sigma_{a_0}$ |
| C' | Constant in Paris equation |
| $C_1$, $C_2$ | Constants in aging time-temperature relationship |
| $C_3(\varepsilon_a)$ | The maximum value of K |
| $C_4(\varepsilon_a)$, $C_5(\varepsilon_a)$ | Constants for a particular strain amplitude |
| d | Half notch width |
| da/dN (DA/DN) | Crack growth rate (in/cycle) |
| $D_o$ | Diffusion coefficient at infinite temperature |
| E | Modulus of elasticity |
| K | $\sigma_y/\sigma_{y_0}$ repeated strain aging; monotonic strength coefficient |
| K' | Cyclic strength coefficient |
| m | Exponent in Paris equation |
| n | Monotonic strain hardening exponent |
| n' | Cyclic strain hardening exponent |
| 2N | Number of reversals, repeated strain aging |
| $2N_f$ (2NF) | Reversals to failure in fatigue |
| R | Universal gas constant; stress ratio in fatigue |
| $S_a$ | Nominal stress amplitude in fatigue of notched members |
| t | Aging time |
| T | Aging temperature |
| x | Ordinate in the direction of diffusion |
| w | Half plate width |

| | |
|---|---|
| $\Delta\varepsilon/2$, $\varepsilon_a$ | Total strain amplitude fatigue |
| $\Delta\varepsilon_e/2$ | Elastic strain amplitude in fatigue |
| $\Delta\varepsilon_p/2$ | Plastic strain amplitude in fatigue |
| $\Delta K$ (DELTA K) | Stress intensity factor range |
| $\Delta H$ | Activation energy |
| $\Delta S/2$ | Nominal stress amplitude in fatigue of notched members |
| $\Delta\sigma$ | Total stress range in fatigue |
| $\Delta\sigma/2$, $\sigma_a$ | Stress amplitude in fatigue |
| $\Delta\sigma_y$ | Increase in yield strength per reversal |
| $\varepsilon_a$ | Applied strain amplitude, repeated strain aging |
| $\varepsilon_p$ | Plastic strain amplitude, repeated strain aging |
| $\varepsilon_r$ | Offset strain in repeated strain aging, $\Delta\sigma_y/E$ |
| $\rho$ | Notch root radius |
| $\sigma_{a_0}$ | Initial cyclic stress amplitude, repeated strain aging |
| $\sigma_f$ | True fracture strength |
| $\sigma_f'$ | Fatigue strength coefficient |
| $\sigma_y$ | Current yield strength, 0.2% offset, repeated strain aging |
| $\sigma_{y_0}$ | Initial yield strength, 0.2% offset, repeated strain aging |
| $\sigma_{y_u}$ | Upper yield point, repeated strain aging |

PART I - REPEATED STRAIN AGING OF SMOOTH SPECIMENS

# I. INTRODUCTION

In annealed or normalized low carbon steels an upper and lower yield point is observed upon straining. Yielding then propagates through the material at the lower yield point by the movement of Lüder's band fronts. Work hardening generally follows the Lüder's band propagation zone (Lüder's strain) on the stress-strain curve.

If the specimen is strained beyond the Lüder's strain, unloaded and immediately retested, the stress-strain curve follows the same path. The stress-strain curve is slightly rounded as yielding occurs and no evidence of upper and lower yield points are found. However, after unloading if the specimen is allowed to age at room temperature for several days or at a higher temperature for a shorter period, then reloaded in the same direction, the discontinuous yielding behavior returns (see Fig. 1). The yield strength now is higher than the flow stress at the end of prestraining. The increase in yield strength on unloading, aging, and reloading is the most universal indication of strain aging and is called "static strain aging."

Strengthening is caused by interstitial solute carbon and nitrogen atoms migrating to dislocations and pinning them. The carbon and nitrogen atoms concentrate at the tensile side of dislocations in the crystal lattice since, in such positions, their energy is minimum.

The amount and type of prestrain determines the extent of increase in yield strength. Prestrains generate fresh dislocations in the specimen. Aging temperature and time treatments allow the carbon and nitrogen to travel to dislocations and lock the fresh dislocations. The existence of many locked dislocations acts as a barrier to their movement upon straining. A higher stress would then be required to move such dislocations. Hence, an increase in yield strength is observed.

Other factors influencing the extent of strengthening are aging temperature and aging time, the type of steel, carbon and nitrogen level in solid solution, microstructure, and the grain size.

A number of studies are reported on static strain aging of steels (1-11).* All of these involve enhancing the yield and tensile strength in the direction of prestraining after various aging treatments.

Wilson et al. (1) examined the early stages of aging and found that the change in yield strength rose slightly as the prestrain was increased from 2 to 7%. They also found that increasing prestrain markedly increased the rate of work hardening and, hence, increased the change in ultimate tensile strength.

The type of prestrain is also an important factor in static strain aging. A return of the yield point requires slightly more aging if a specimen is prestrained in tension, aged and restrained in compression and vice versa. Various theories have been suggested to explain this phenomenon. These theories discuss the gradual relaxation of microstresses and the relaxation of the Bauschinger effect. If a specimen is restrained in a direction other than the original prestrain direction, most of the dislocations will be free to move away from the obstacles that are blocking them. It is after the isolated dislocations in the restraining direction get locked that a yield point can be reobserved and enhanced.

The effect of aging temperature is also studied (2). Aging temperatures in the range 15-250°C do not alter appreciably the properties in the fully

---

*Numbers in parentheses refer to the list of references following the text.

aged condition. The main effect of increasing the aging temperature is to accelerate the approach to the fully aged condition. Sufficient aging time is required to allow the interstitial atoms to diffuse and pin the dislocations. If the temperature during the aging period is raised, the carbon and nitrogen can diffuse at faster rates. Less time would then be required for the return of the yield point.

The amount of carbon and nitrogen in solid solution has an effect on the strain aging behavior. Heat treatments that increase the carbon and nitrogen in solid solution increase strain aging. Coarse grained steels are known to be less sensitive to strain aging than fine grained steel.

If prestraining in tension, aging and restraining in the same direction is done repeatedly, the process is called repeated strain aging. This type of strain aging results in a higher yield strength compared to single step strain aging. Repeated reversals of strain in one direction create large numbers of dislocations that become pinned after temperature-time treatments. Upon restraining an increase in yield strength is observed.

Little previous work in this field has been done. Edwards et al. (2) have reported results that show that aging after 2-3% tensile strain increments results in a larger increase in yield and tensile strength than loading to the same total strain and then aging fully.

Hundy and Boxall (3) examined the effect of cold working operations on the yield and tensile strength. They showed that if the steel is given several cold working passes and aged only after the final pass, the total change in tensile and yield strength is less than if the steel had been aged after each pass.

"Repeated strain aging" technique introduced in this study involves applications of tensile plastic strain followed by aging at zero load, then compressive plastic strain followed by aging. As this procedure is continued, it results in an equal enhancement of strength in tension and compression.

Little work has been done in the fatigue behavior of statically strain aged specimens. Mintz et al. (12) found that 5% tensile prestrain followed by aging at 250°C-300°C gave no improvement in completely reversed stress control tests.

Sandor (13) found that frequent aging treatments during stress control tests reduced the plastic strain and increased the fatigue life. He noted that the fatigue damage process is retarded due to temporary pinning of dislocations by carbon and nitrogen atoms causing strengthening of the material.

An increase in fatigue life is observed when low carbon steels are cycled at elevated temperatures in the long life region (14). This is due to dynamic strain aging effects where strengthening occurs by pinning of dislocations by solute atoms during fatigue. Dynamic strain aging effects have been studied by various investigators (15-18) on different steels.

The effect of strain aging on fatigue crack initiation in steel is reviewed by Wilson (19) based on the limited experimental data in the literature. Both dynamic strain aging and static strain aging effects are discussed with emphasis on microstructural changes during fatigue.

# II. EXPERIMENTAL PROGRAM

## A. Material, Specimen and Equipment

Commercially available, ASTM A-36 (hot rolled bar and hot rolled strip) steel is used throughout this study. The diameter of the rolled bars was 3/4 in. Chemical composition and monotonic properties of the ASTM A-36 (hot rolled bar) are given in Table I.

Tests were performed on a 22 kip MTS materials test system interfaced to a multiuser PDP 11/34 digital computer. This allows for computer controlled tests with stress-strain data acquisition.

A Lepel induction heating system with a 2.5 kw induction generator was used to heat the specimen. An optimum induction coil design was used which minimized the specimen's thermal gradient. In such a system, heating occurs by circumferential eddy currents induced in the specimen by high frequency currents that flow in the coil surrounding the specimen. Thermocouples were spot welded to the specimen for use as feedback to the temperature controller. Specimens were cooled to room temperature with compressed air. A high temperature MTS axial extensometer with quartz knife-edges and with 1 in. gage length was used.

Stainless steel grips that were water cooled to protect the load cell were used. The specimen was attached to the hydraulic ram through a liquid-solid Wood's metal grip to reduce clamping distortions.

## B. Aging Time-Temperature Relationship for the Recovery of the Upper Yield Point

Tests were conducted to obtain a relationship between equivalent aging times and temperatures required for the recovery of the upper yield point (8% yield drop).

Specimens were strained in tension and aged at zero load at a fixed temperature for a certain aging time. The aging time was gradually increased until an upper yield point is recovered (8% yield drop) upon restraining. The time, t, at which such a recovery is observed is taken as the correct aging time for that temperature. This procedure was repeated at different temperature levels and similarly correct aging times were established.

Aging times greater than t for a particular temperature do not significantly change the recovery behavior as the aging reactions are completed.

Throughout the repeated strain aging tests, aging times and temperatures were selected that permitted complete recovery of the upper yield point.

C. Repeated Strain Aging Tests

Repeated strain aging tests involve the application of positive and negative plastic strain reversals to the specimen with aging periods at zero load.

The specimen was strained in the tensile direction to a strain amplitude of $\varepsilon_a$ then unloaded to zero load (see Fig. 3). At zero load there exists a tensile plastic strain $\varepsilon_p$ (position 1). The specimen was then aged at 250°C for four minutes at zero load. Compressed air was used to cool the specimen to ambient temperature.

The specimen was then strained in the compressive direction to the same strain amplitude, $\varepsilon_a$. Upon unloading to zero a tensile strain, $\varepsilon_r$, close to zero strain was reached. If the yield point in compression is enhanced by an amount $\Delta\sigma_y$, the strain, $\varepsilon_r$, would deviate from zero by an amount $\Delta\sigma_y/E$ (position 2). Aging follows at zero load.

This sequence is repeated. Repeated strain reversals are applied until nearly full strengthening is observed. Figure 4 shows the positive and negative strain reversals with aging periods at zero load. Below the strain reversals, the applied temperature cycles are shown in the same figure.

D. Fatigue Tests

Constant amplitude, totally reversed, strain controlled fatigue tests were performed on repeatedly strain aged and unaged specimens. All tests were performed at room temperature in laboratory air.

# III. EXPERIMENTAL RESULTS

## A. Aging Time-Temperature Relationship Results for the Recovery of the Upper Yield Point

Table II shows the results of aging time and temperature for the recovery of the upper yield point with 8% yield drop. The results are plotted in Fig. 5. The relationship is of the form (see Appendix).

$$\log_{10} t^{-1} = \log_{10}(2D_o x^{-2}) - \frac{\Delta H}{RT} \log_{10} e \qquad (1)$$

where:

$D_o$ = diffusion coefficient at infinite temperature ($cm^2$/sec)

$\Delta H$ = activation energy for the process (cal/mol)

R = universal gas constant (= 1.986 (cal/°K)/mol)

T = absolute temperature (°K)

t = time for diffusion (secs)

x = ordinate in the direction in which diffusion occurs (cm)

For particular values of x, $\Delta H$, $D_o$:

$$\log_{10} t^{-1} = C_1 - \frac{C_2}{T} \qquad (2)$$

where $C_1$ and $C_2$ are constants.

Linear regression analysis on the results shown on Fig. 5 gives,

$$\log_{10} t^{-1} = 7 - \frac{4296}{T} \qquad (3)$$

The activation energy for the process can be calculated using Eqs. 1 and 3.

$$\frac{\Delta H}{R} \log_{10} e = 4296 \qquad (4)$$

Equation 4 gives,

$$\Delta H = 19{,}600 \text{ cal/mol}$$

This value is between the activation energy for diffusion of C in iron (20,100 cal/mol) and N in iron (18,200 cal/mol).

B. Repeated Strain Aging Tests Results

Repeated strain aging tests were carried out at different strain amplitudes, $\varepsilon_a$. Figures 6 and 7 show the yield strength ratio K in tension and compression versus the number of reversals. The yield strength ratio at a certain number of reversals is defined as the current yield strength over the yield strength of the unaged material. At the first reversal the yield strength ratio is unity.

The relationship between K and the number of reversals, 2N, can be approximated by the following relationship.

$$K = C_3(\varepsilon_a) - C_4(\varepsilon_a)\exp(-2N\ C_5(\varepsilon_a)) \qquad (5)$$

where

$C_3(\varepsilon_a)$ = the maximum value of $\sigma_y/\sigma_{y_o}$ reached (depends on strain amplitude)

$C_4(\varepsilon_a)$, $C_5(\varepsilon_a)$ = a constant for a particular strain amplitude

2N = number of reversals

Figures 8 and 9 show the cyclic stress amplitude ratio versus number of reversals in tension and compression. The cyclic stress amplitude, $\sigma_a$, is defined as the stress corresponding to the applied strain amplitude (maximum strain), $\varepsilon_a$. The cyclic stress amplitude ratio at a certain number of reversals is the ratio of the current cyclic stress amplitude over the cyclic stress amplitude of the unaged material, both measured at the maximum strain amplitude.

The increase in cyclic stress amplitude ratio is an indication of the work hardening behavior of the material. Its increase is related to an increase in ultimate tensile strength. The relationship between the value of C and 2N can be approximated by an expression similar to Eq. 5. However, the cyclic stress amplitude ratio reaches a higher asymptotic value than the yield strength ratio.

The decrease in plastic strain, $\varepsilon_p$, with number of reversals is plotted in Figs. 10(a), 10(b), 10(c). The decrease in plastic strain is an indication of the hardening of the material.

C. Fatigue Test Results

Table III shows the results of constant amplitude strain controlled tests (sine waveform) on the ASTM A-36 hot rolled strip tested by Deves (20). Table IV shows the results of similar tests on the ASTM A-36 hot rolled bar which are repeatedly strain aged. Figure 11 compares the strain-life data for both cases.

The monotonic and cyclic properties of the ASTM A-36 (hot rolled strip) are given on Tables V and VI.

Data on repeatedly strain aged specimens under fatigue show that cyclic stability is not reached except for tests in the long life region.

The fatigue life of unaged specimens at 0.15% strain amplitude was approximately 600,000 cycles. At the same amplitude the repeatedly strain aged specimen did not fail in two million cycles.

At amplitudes above 0.15%, the fatigue life of unaged specimens is superior to repeatedly strain aged specimens. Repeatedly strain aged samples tend to show delayed cyclic softening leading to cyclic plastic strains that increase with number of cycles.

## IV. DISCUSSION OF RESULTS

"Repeated strain aging" technique introduced here produces an increase in both tensile and compressive yield strength and cyclic stress amplitude at the maximum strain. With each reversal a higher dislocation density is generated. Aging treatments allow the interstitial carbon and nitrogen atoms to form atmospheres and lock dislocations. With repeated strain aging, locked dislocations are established in tension and compression directions.

Prestraining in any direction will then result in dislocations pressing against locked dislocation tangles. Therefore, repeated strain aging gives rise to an equal enhancement of the yield strength in tension and compression and the elimination of the Bauschinger effect.

Atmosphere formation (locking) saturates after each dislocation has attracted a certain number of solute atoms per atom plane. Carbon and nitrogen in excess is believed to diffuse along the dislocation line and form precipitates. The yield strength increases during both of the above stages. However, it appears that the precipitates formed are primarily responsible for the increase in cyclic stress amplitudes and work hardening rates.

Strain aging takes place more rapidly the larger the strain amplitude (Figs. 6, 7, 8, 9). Fewer reversals are required to achieve the maximum yield strength as the strain amplitude increases. At high strain amplitudes atmosphere locking is completed at an early stage and precipitate diffusion; hence, work hardening dominates during repeated strain aging. The cyclic stress amplitudes corresponding to the maximum strain achieved at later stages of strain aging are higher than the ultimate tensile strength of the unaged material. The maximum value of the tensile cyclic stress amplitude achieved was 665 MPa. The ultimate tensile strength of the unaged material is approximately 500 MPa from monotonic tensile tests (see Table I).

For strain amplitudes less than the Lüder's strain, there exists a short delay in increase in yield strength due to formation of yielded and unyielded regions (Fig. 6). When the unyielded regions are consumed after several strain reversals, the yield strength ratio increases.

The plastic strain amplitude (Figs. 10(a), 10(b), 10(c)) reduces after each reversal, saturating to a constant value in the later stages of aging.

The net plastic strain imposed on the specimen as a result of strain reversals in both tension and compression is nearly zero. Conventional strain aging methods impose permanent sets on the material that may be unacceptable for designs with tight tolerances. Besides, in such cases the residual ductility may be lowered.

The results of strain-controlled fatigue tests on repeatedly strain aged and unaged specimens are shown in Fig. 11. Repeatedly strain aged specimens were found to cyclically soften at strain amplitudes above 0.15% and showed no cyclic stability. The stress amplitude reached a stable value only for tests below 0.15% strain amplitude. The stable stress at this strain amplitude was 280 MPa in aged specimens and 240 MPa for unaged samples.

# PART 2 - REPEATED STRAIN AGING OF NOTCHED MEMBERS

## I. EXPERIMENTAL PROGRAM

### A. Material, Specimen and Equipment

The material used in this part of the study is an ASTM A-36 steel (hot rolled strip). The chemical composition of the material is shown on Table V. The monotonic and cyclic stress-strain properties of this material were determined by Deves (20) from smooth specimens cut from the hot rolled strip and are shown in Tables V and VI. Table VII gives the results of strain controlled fatigue tests. Figures 12 and 13 show the stress-strain curve (monotonic and cyclic) and the strain-life curve of the material.

The notched plates tested were cut from the hot rolled strip and were 0.225 in. thick, 2 in. wide and 11 in. long. The specimen length inside the collet grips was 7 in. Two notch geometries were used. Figure 14 shows the plate with a 0.3 in. diameter hole at the center. Figure 15 shows the plate with a slot 0.3 in. long and 0.15 in. wide at the center.

Circular notched plates were tested in a 50 kip and slot notched plates were tested in a 22 kip closed loop computer controlled materials testing (MTS) system.

A heating tape was used to heat the specimens during aging. Thermocouples in contact with the specimen provided the means of temperature measurement. The heating tape was removed prior to fatigue testing. The specimen was cooled to room temperature with compressed air. Cracks were measured by a replicating technique. Small cracks up to 0.001 in. were detected with this method.

### B. Experimental Procedure

Repeated strain aging of notched members involve stress reversals in tension followed by aging at zero nominal load followed by a stress reversal in compression (Fig. 16). As this procedure is continued the yield strength of the material at the notch root increases with reversals (Fig. 17). The nominal stresses applied were increased slightly after each reversal to maintain the notch root strain at an approximately constant value. The nominal stresses applied at each reversal was determined from smooth specimen (repeated strain aging) data (Figs. 6-9) and using Neuber's rule (21-22).

The last reversal applied was in compression. This should result in a residual tensile stress at the notch root.

After the above procedure is completed the notched member is subjected to load control fatigue testing (R = -1). The results are compared with fatigue tests on unaged notched plates of the same material and geometry. Crack initiation and propagation behavior were compared in both cases.

Cracks were measured in strain aged and unaged slot notched plates. The data are presented as crack length, a, versus number of cycles, N. Cyclic crack growth rates were determined from a versus N data by an incremental polynomial procedure. A second order polynomial was fitted through the first seven a versus N data points using least squares regression analysis. The first derivative of this polynomial was then evaluated at the central data point to obtain a crack growth rate, da/dN. This procedure was applied to subsequent data points to obtain crack growth rates at various number of cycles.

The stress intensity factor range for finite width notched plates from linear elastic fracture mechanics can be expressed in the form:

$$\Delta K = \Delta S\sqrt{\pi a}\; F\left(\rho, \frac{d}{w}, \frac{a}{w}\right)$$

where

$\rho$ = notch root radius

d = half notch width

w = half plate width

The correction factors were estimated by interpolation from Tada et al. (23) and Newman (24) within 5% accuracy.

Fatigue crack propagation characteristics are most frequently represented in the form of a power law (25).

$$\frac{da}{dN} = C'(\Delta K)^m$$

Using linear regression analysis a straight line in log-log coordinates is fitted to the unaged slot notched plate data to obtain the coefficient C' and the exponent m.

## II. EXPERIMENTAL RESULTS

Table VII shows the results of fatigue tests ($R = -1$) on circular notched plates. The results are plotted in Fig. 18. Table VIII shows the results of fatigue tests ($R = -1$) on slot notched plates. Reversals to a crack length of 0.025 in. and failure are plotted as Figs. 19 and 20. Figures 21 to 23 show the relationship between the measured crack length, a, and the number of cycles, N, in slot notched plates at three different stress levels. Crack growth rate, da/dN (inch/cycle), versus stress intensity factor range, $\Delta K(\text{ksi}\sqrt{\text{in}})$, is plotted in Fig. 24 for the three stress levels. Strain aged and unaged specimens were compared in all cases.

For growth rates in the range $10^{-4}$ to $3 \times 10^{-7}$ inch/cycle the linear log-log equation that best fits the unaged slot notched plate data is (Fig. 25)

$$\frac{da}{dN} - 2.7 \times 10^{-11}(\Delta K)^{4.12}$$

# III. DISCUSSION OF RESULTS

Results indicate that repeated strain aging improves the fatigue life of notched members in the long life region by extending the period of crack initiation. Only slight improvement in fatigue life is observed in repeatedly strain aged members at other stress levels. Crack propagation life and da/dN versus $\Delta K$ characteristics of the material are unaltered by repeated strain aging.

## CONCLUSIONS

1. Repeated strain aging eliminates the Bauschinger effect and results in equal enhancement of the tensile and compressive yield strength.
2. Increase in yield strength of smooth specimens was from 350 MPa to 544 MPa (55%) at the end of repeated strain aging. Cyclic stress amplitude (corresponding to the maximum strain amplitude) increased between 55-95% depending on the strain amplitude.
3. The repeated strain aging technique used in this investigation imposes no permanent set on the specimen at the conclusion of full strengthening hence is feasible for use on components with tight dimensional tolerances.
4. Only slight improvements in the long-life fatigue performance is obtained in smooth specimens repeatedly strain aged prior to fatigue testing.
5. Selective strengthening of notched members by repeated strain aging is beneficial at long lives.
6. At high stress levels the effect of repeated strain aging is almost negligible in notched members.

REFERENCES


1. Wilson, D. V. and Russell, B., "The Contribution of Precipitation to Strain Aging of Low Carbon Steels," Acta Metallurgica, Vol. 8, 1960, pp. 468-479.

2. Edwards, C. A., Jones, H. N. and Walters, B., "A Study of Strain-Age Hardening of Mild Steel," J. of Iron and Steel Inst., No. 139, 1939, pp. 341-385.

3. Hundy, B. B. and Boxall, T. D., "The Repeated Strain Aging of Mild Steel," Metallurgia, 54, 1957, pp. 27-30.

4. Tardif, N. P. and Ball, C. S., "The Effect of Temper-Rolling on the Strain Aging of Low Carbon Steel," J. of Iron and Steel Inst., No. 182, 1956, pp. 9-19.

5. Wilson, D. V. and Russell, B., "The Contribution of Atmosphere Locking to the Strain Aging of Low Carbon Steels," Acta Metallurgica, Vol. 8, 1960, pp. 36-45.

6. Haasen, P., "Interaction of Dislocations and Foreign Atoms," Proceedings of the Symposium on Internal Stresses and Fatigue in Metals, Detroit, 1959, Elsevier Publishing Co., pp. 205-219.

7. Fisher, D. H., Carlson, R. L. and Lankford, W. T., "The Effects of Strain Rate and Temper-Rolling on the Strain-Aging Characteristics of Rimmed Deep-Drawing Steel," Proceedings ASTM, No. 48, 1958, pp. 932-942.

8. Rashid, M. S., "Strain Aging of V. N. T. Strengthened Low-Alloy Steels," Metallurgical Transactions, Vol. 6A, 1973, pp. 1265-2168.

9. Baird, J. D., "Strain Aging of Steel--A Critical Review," Iron and Steel, No. 36, 1963, pp. 186-192.

10. Ibid, pp. 368-374.

11. Ibid, pp. 400-405.

12. Mintz, B. and Wilson, D. V., "Fatigue Behavior of a Heat Treated Alloy Steel," J. of Iron and Steel Inst., Vol. 204, 1966, pp. 91-94.

13. Sandor, B. I., "Metal Fatigue with Elevated Temperature Rest Periods," Ph.D. Thesis, Department of Theoretical and Applied Mechanics, University of Illinois, Urbana, Illinois, 1968.

14. Levy, J. C. and Sinclair, G. M., "An Investigation of Strain Aging in Fatigue," TAM Report No. 39, University of Illinois, Urbana, Illinois, 1954.

15. Coffin, L. F., Jr., "The Effect of Quench Aging and Cyclic-Strain Aging on Low Carbon Steel," J. of Basic Engineering, Transactions of ASME, June, 1965, pp. 351-362.

16. Nakagawa, T. and Ikai, Y., "Strain Aging and the Fatigue Limit in Carbon Steel," Fatigue of Engineering Materials and Structures, Vol. 2, No. 1, 1979, pp. 13-21.

17. Abdel-Raouf, H., Plumtree, A. and Topper, T. H., "Effects of Temperature and Deformation Rate on Cyclic Strength and Fracture of Low-Carbon Steel," ASTM STP 519, 1973, pp. 28-57.

18. Rally, F. C. and Sinclair, G. M., "Influence of Strain Aging on the Shape of the S-N Diagram," TAM Report No. 87, University of Illinois, Urbana, Illinois, 1955.

19. Wilson, D. V., "Effects of Microstructure and Strain Aging on Fatigue Crack Initiation in Steel," Metal Science, Vol. 11, 1977, pp. 321-331.

20. Deves, T. J., "The Effect of Small Amplitude Subcycles in Variable Amplitude Block Loading Histories," M.S. Thesis, Department of Theoretical and Applied Mechanics, University of Illinois, Urbana, Illinois, 1981.

21. Neuber, H., "Theory of Stress Concentration for Shear Strained Prismatical Bodies with Arbitrary Nonlinear Stress Strain Law," J. of Applied Mechanics, Transactions of ASME, December, 1961, pp. 544-550.

22. Neuber, H., "Theory of Notch Stresses, Principles for Exact Stress Calculations," J. N. Edwards, Ann Arbor, Michigan, 1946.

23. Tada, H., Paris, P. C. and Irwin, G. R., The Stress Analysis of Cracks Handbook, Del Research Corporation, Hellertown, Pennsylvania, 1973.

24. Newman, J. C., "An Improved Method of Collocation for the Stress Analysis of Cracked Plates with Various Shaped Boundaries," NASA TN D-6376, August, 1971.

25. Paris, P. C., "The Fracture Mechanics Approach to Fatigue," Fatigue an Interdisciplinary Approach, Proceedings of the Tenth Sagamore Conference, Syracuse University Press, 1963, pp. 107-132.

26. Cottrell, A., Dislocations and Plastic Flow in Crystals, Oxford Press, 1953.

27. Honeycombe, R. W. K., The Plastic Deformation of Metals, Edward Arnold, 1968.

# APPENDIX

Considering the diffusion of interstitial atoms to dislocation, the order of time to achieve equilibrium in the direction in which diffusion occurs, x, has been given (14) as

$$t = \frac{x^2}{2D} \quad (1a)$$

where

x = ordinate coinciding with the direction in which diffusion occurs (cm)

D = diffusion coefficient ($cm^2/sec$)

The diffusion coefficient at any temperature is given in terms of the coefficient at infinite temperature.

$$D = D_o \exp(-\Delta H/RT) \quad (2a)$$

where

$D_o$ = diffusion coefficient at infinite temperature ($cm^2/sec$)

$\Delta H$ = activation energy for the process (cal/mol)

R = universal gas constant (= 1.986 (cal/°K)/mol)

T = absolute temperature (°K)

Substituting Eq. 2a into Eq. 1a

$$t^{-1} = \frac{2D}{x^2} = 2D_o\ x^{-2}\ e^{-\Delta H/RT} \quad (3a)$$

or

$$\log_{10} t^{-1} = \log_{10}(2D_o\ x^{-2}) - \frac{\Delta H}{RT} \log_{10} e \quad (4a)$$

and for a particular x, $\Delta H$ and $D_o$:

$$\log_{10} t^{-1} = C_1 - \frac{C_2}{T} \quad (5a)$$

where $C_1$ and $C_2$ are constants.

TABLE I

MATERIAL PROPERTIES

Designation: ASTM A-36 Hot Rolled Bar

Chemistry (w/o): (Average of several tests)

| C | Mn | P | S | Si | Cr | Ni | Mo | Cu | Aℓ | Sn |
|---|---|---|---|---|---|---|---|---|---|---|
| 0.26 | 0.75 | 0.004 | 0.028 | 0.15 | 0.09 | 0.09 | 0.03 | 0.14 | 0.005 | 0.011 |

Monotonic Properties:

| | |
|---|---|
| Modulus of Elasticity, E | 30,500 ksi (210,000 MPa) |
| Yield Strength, 0.2% $S_y$ | 50.75 ksi (350 MPa) |
| Ultimate Strength, $S_u$ | 73 ksi (504 MPa) |
| Reduction in Area, %RA | 65% |
| True Fracture Strength, $\sigma_f$ | 158.5 ksi (1,092 MPa) |
| True Fracture Ductility, $\varepsilon_f$ | 1.05 |
| Strain Hardening Exponent, n | 0.235 |
| Strength Coefficient, K | 143.5 ksi (989 MPa) |
| Lüder Strain, % | 1.7 |

TABLE II

AGING TIME-TEMPERATURE RELATIONSHIP
FOR THE RECOVERY OF THE UPPER YIELD POINT

| Aging Temperature, T (°K) | Aging Time, t (Secs) | 1000/T | $Log_{10}\ t^{-1}$ | $\frac{\sigma_{y_u} - \sigma_{y_o}}{\sigma_{y_u}} \times 100$ (%) |
|---|---|---|---|---|
| 383 | 11,400 | 2.61 | -4.057 | 8.0 |
| 423 | 3,600 | 2.36 | -3.556 | 8.0 |
| 473 | 60 | 2.11 | -1.778 | 8.5 |
| 523 | 20 | 1.91 | -1.301 | 8.0 |

TABLE III

RESULTS OF CONSTANT AMPLITUDE STRAIN-CONTROLLED TESTS (SINE WAVEFORM), MATERIAL: A-36 HOT ROLLED STRIP

| $\Delta\varepsilon/2$ | $2N_f$ | $\Delta\sigma/2$ (ksi) |
|---|---|---|
| $0.01^{\dagger}$ | 2,477 | 60.4 (417 MPa) |
| 0.0075* | 4,749 | 58.3 (402 MPa) |
| $0.005^{+}$ | 15,250 | 51.3 (354 MPa) |
| $0.004^{+}$ | 27,476 | 47.15 (325 MPa) |
| $0.003^{\dagger}$ | 65,235 | 39.9 (275 MPa) |
| $0.002^{\dagger}$ | 250,260 | 36.2 (250 MPa) |
| $0.0015^{+}$ | $1.26 \times 10^6$ | 34.5 (238 MPa) |
| 0.001 | $2.1 \times 10^6$ | 31.0 (213 MPa) |

$^{+}$Indicates average of two tests.

$^{\dagger}$Indicates average of three tests.

*Indicates average of five tests.

TABLE IV

RESULTS OF CONSTANT AMPLITUDE STRAIN-CONTROLLED TESTS (SINE WAVEFORM),
MATERIAL: A-36 HOT ROLLED BAR, REPEATEDLY STRAIN AGED

| $\Delta\varepsilon/2$ | $2N_f$ | $\Delta\sigma/2$ (ksi) |
|---|---|---|
| 0.003 | 32,000 | 42.78* (295 MPa) |
| 0.002 | 136,400 | 41.55* (287 MPa) |
| 0.002 | 176,000 | 38.43* (265 MPa) |
| 0.0015 | @ 4 x $10^6$ No failure | 40.6 (280 MPa) |

*Indicates stress level before failure, no cyclic stability.

TABLE V

MATERIAL PROPERTIES

Designation: ASTM A-36 Hot Rolled Strip

Chemistry (w/o): (Average of several tests)

| C | Mn | P | S | Si | Ni | Cr | Mo | Cu | B | V |
|---|---|---|---|---|---|---|---|---|---|---|
| 0.25 | 0.83 | 0.01 | 0.025 | 0.255 | 0.10 | 0.09 | 0.01 | 0.016 | Nil | Nil |

Hardness: 140 BHN(80 $R_b$)

Monotonic Properties: (Average of two tests)

| | |
|---|---|
| Modulus of Elasticity, E | 30,500 ksi (210,000 MPa) |
| Yield Strength, 0.2% $S_y$ | 50.9 ksi (351 MPa) |
| Ultimate Strength, $S_u$ | 78.3 ksi (540 MPa) |
| Reduction in Area, %RA | 66.8% |
| True Fracture Strength, $\sigma_f$ | 170.1 ksi (1,173 MPa) |
| True Fracture Ductility, $\varepsilon_f$ | 1.10 |
| Strain Hardening Exponent, n | 0.236 |
| Strength Coefficient, K | 144 ksi (992 MPa) |

## TABLE VI

## CYCLIC PROPERTIES

From Constant Amplitude Strain Controlled Tests:
(Ramp Waveform)

| | |
|---|---|
| Modulus of Elasticity, E | 29,000 ksi (200,000 MPa) |
| Yield Strength, 0.2% $S_y$ | 47.86 ksi (330 MPa) |
| Strain Hardening Exponent, n' | 0.226 |
| Strength Coefficient, K' | 193.8 ksi (1,336 MPa) |
| Fatigue Strength Coefficient, $\sigma_f'$ | 162 ksi (1,118 MPa) |
| Fatigue Ductility Coefficient, $\varepsilon_f'$ | 0.338 |
| Fatigue Strength Exponent, b | -0.110 |
| Fatigue Ductility Exponent, c | -0.480 |
| Transition Fatigue Life, $2N_t$ | 90,000 rev |

TABLE VII

RESULTS OF CONSTANT AMPLITUDE STRAIN-CONTROLLED TESTS (RAMP WAVEFORM).
MATERIAL: A-36 HOT ROLLED STRIP

| Specimen No. | Total Strain Amp., $\Delta\varepsilon/2$ | Plastic Strain Amp., $\Delta\varepsilon_p/2$ | Elastic Strain Amp., $\Delta\varepsilon_e/2$ | Stress Amp., $\Delta\sigma/2$ (ksi) | Reversals to Failure $2N_f$ |
|---|---|---|---|---|---|
| 92 | 0.0010 | $< 10^{-5}$ | 0.00100 | 29.88 (206 MPa) | No failure |
| 48 | 0.0018 | 0.00053 | 0.00130 | 37.4 (258 MPa) | No failure @ $4 \times 10^6$ |
| 26 | 0.00202 | 0.00081 | 0.00121 | 37.85 (261 MPa) | 359,690 |
| 84 | 0.00202 | 0.00070 | 0.00132 | 37.85 (261 MPa) | 416,714 |
| 35 | 0.00306 | 0.00160 | 0.00146 | 44.23 (305 MPa) | 65,653 |
| 36 | 0.00410 | 0.00239 | 0.00171 | 49.31 (340 MPa) | 25,221 |
| 38 | 0.00510 | 0.00323 | 0.00187 | 53.9 (372 MPa) | 15,894 |
| 76 | 0.00509 | 0.00322 | 0.00187 | 52.6 (363 MPa) | 11,869 |
| 80 | 0.00510 | 0.00322 | 0.00188 | 53.52 (369 MPa) | 15,948 |
| 39 | 0.00756 | 0.00552 | 0.00204 | 58.6 (404 MPa) | 5,119 |
| 41A | 0.0102 | 0.00783 | 0.00224 | 62.1 (428 MPa) | 2,671 |
| 82 | 0.0102 | 0.00784 | 0.00232 | 63.8 (440 MPa) | 2,952 |
| 94 | 0.0131 | 0.0107 | 0.00241 | 63.8 (440 MPa) | 1,175 |
| 97 | 0.0132 | 0.0107 | 0.00253 | 62.65 (432 MPa) | 1,725 |
| 96 | 0.0151 | 0.0125 | 0.00259 | 64.39 (444 MPa) | 989 |

TABLE VIII

RESULTS OF FATIGUE TESTS (R = -1) ON NOTCHED SPECIMENS
GEOMETRY: CIRCLE MATERIAL: ASTM A-36 HOT ROLLED STRIP

| Specimen No. | Stress† Amplitude $\Delta S/2$ ksi | Reversals to Failure $2N_f$ |
|---|---|---|
| 8 | 16.99 | 2,361,400 |
| 14 | 17.38 | 7,600,000* |
| 3 | 18.3 | 1,179,020 |
| 18 | 19.0 | 3,560,000* |
| 7 | 19.6 | 849,500 |
| 5 | 20.92 | 460,920 |
| 17 | 23.53 | 258,000 |
| 3 | 23.53 | 395,240* |
| 14A | 26.14 | 103,920 |
| 9 | 26.14 | 166,800* |
| 4 | 32.67 | 26,680 |
| 1 | 39.2 | 5,600 |
| 2 | 39.2 | 7,206 |

*Indicates repeatedly strain aged specimens.

†All stresses are nominal.

TABLE IX

RESULTS OF FATIGUE TESTS (R = -1) ON NOTCHED SPECIMENS
GEOMETRY: SLOT MATERIAL: A-36 HOT ROLLED STRIP

| Specimen No. | Stress[+] Amplitude $\Delta S/2$ (ksi) | Reversals to $a = 0.025''$ $2N$ | Reversals to Failure $2N_f$ |
|---|---|---|---|
| 1 | 15.65 | --- | 1,326,000 |
| 2 | 16.09 | --- | 3,862,000* |
| 4† | 16.51 | 340,000 | 886,000 |
| 5† | 16.51 | 880,000 | 1,300,000* |
| 6A | 20.0 | --- | 386,000 |
| 7† | 20.0 | 174,630 | 430,000 |
| 8† | 20.0 | 410,000 | 606,000* |
| 11† | 25.0 | 50,000 | 128,000 |
| 12 | 25.0 | --- | 130,800 |
| 3† | 28.44 | 28,000 | 65,000 |
| 6† | 28.44 | 35,600 | 78,000* |
| 9† | 35.0 | 10,800 | 19,800 |
| 10† | 40.0 | 4,800 | 7,660 |
| 13† | 45.0 | 1,848 | 2,120 |

†Indicates specimens where cracks were measured with a replicating technique.

*Indicates repeatedly strain-aged specimens.

[+]All stresses are nominal.

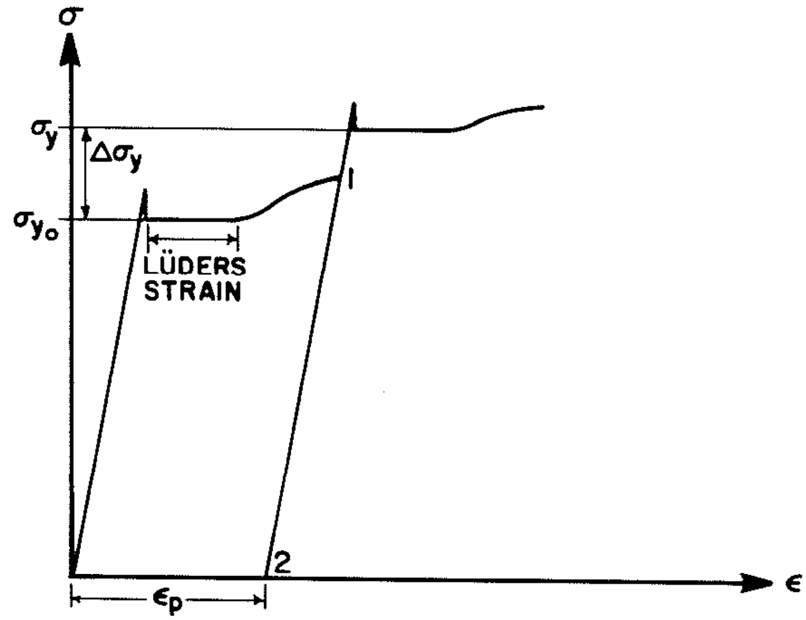


FIG. 1 STRESS-STRAIN CURVE OF A NORMALIZED STEEL UNDER STATIC STRAIN AGING

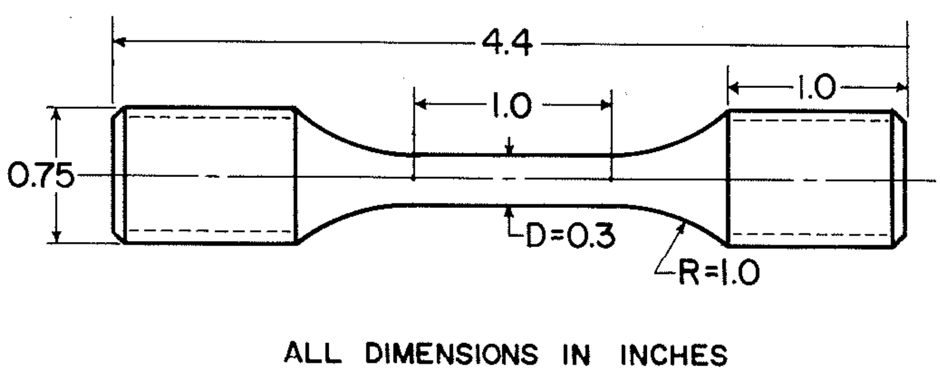


FIG. 2 SMOOTH TEST SPECIMEN

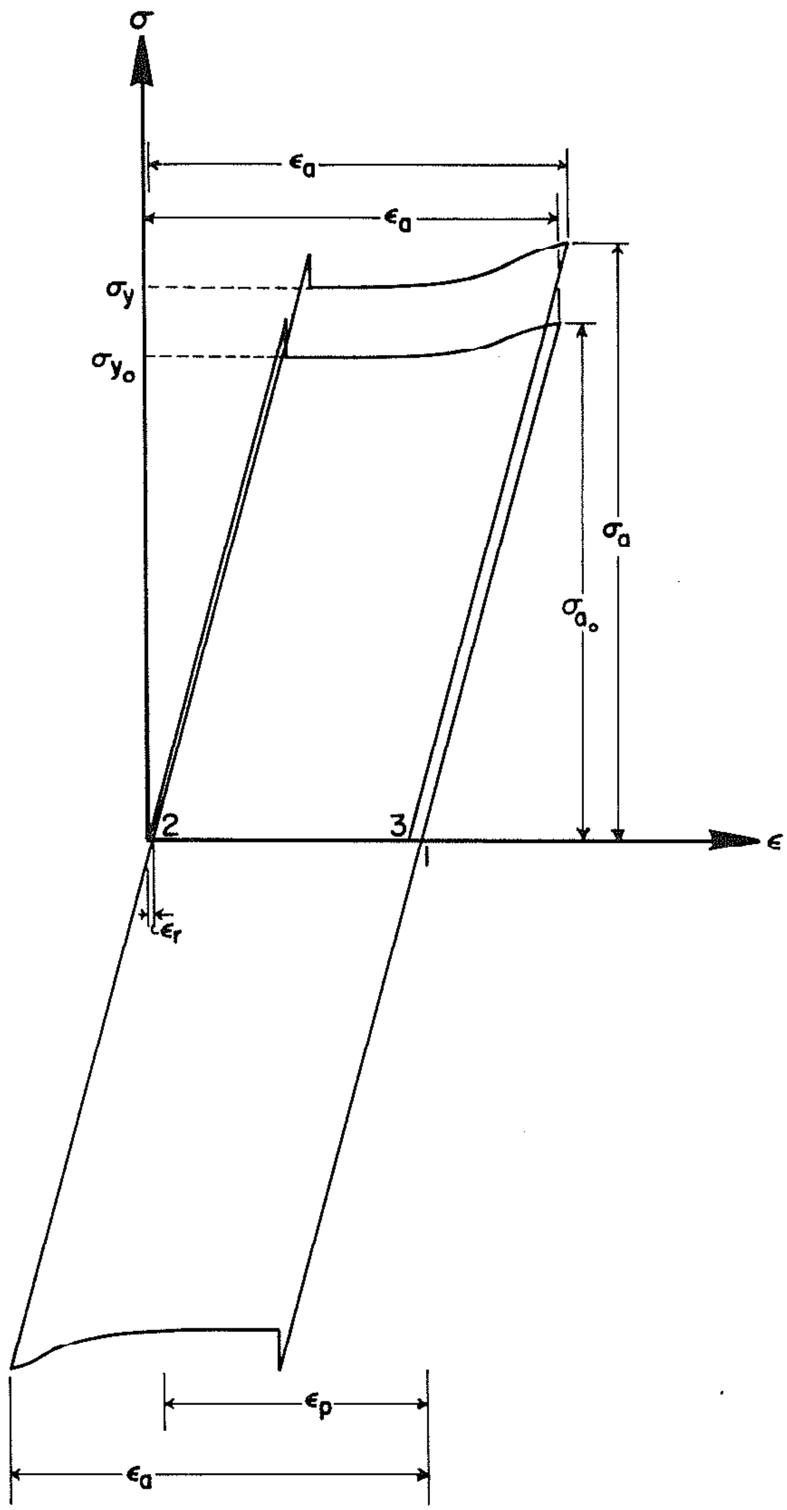


FIG. 3 REPEATED STRAIN AGING STRESS-STRAIN RESPONSE

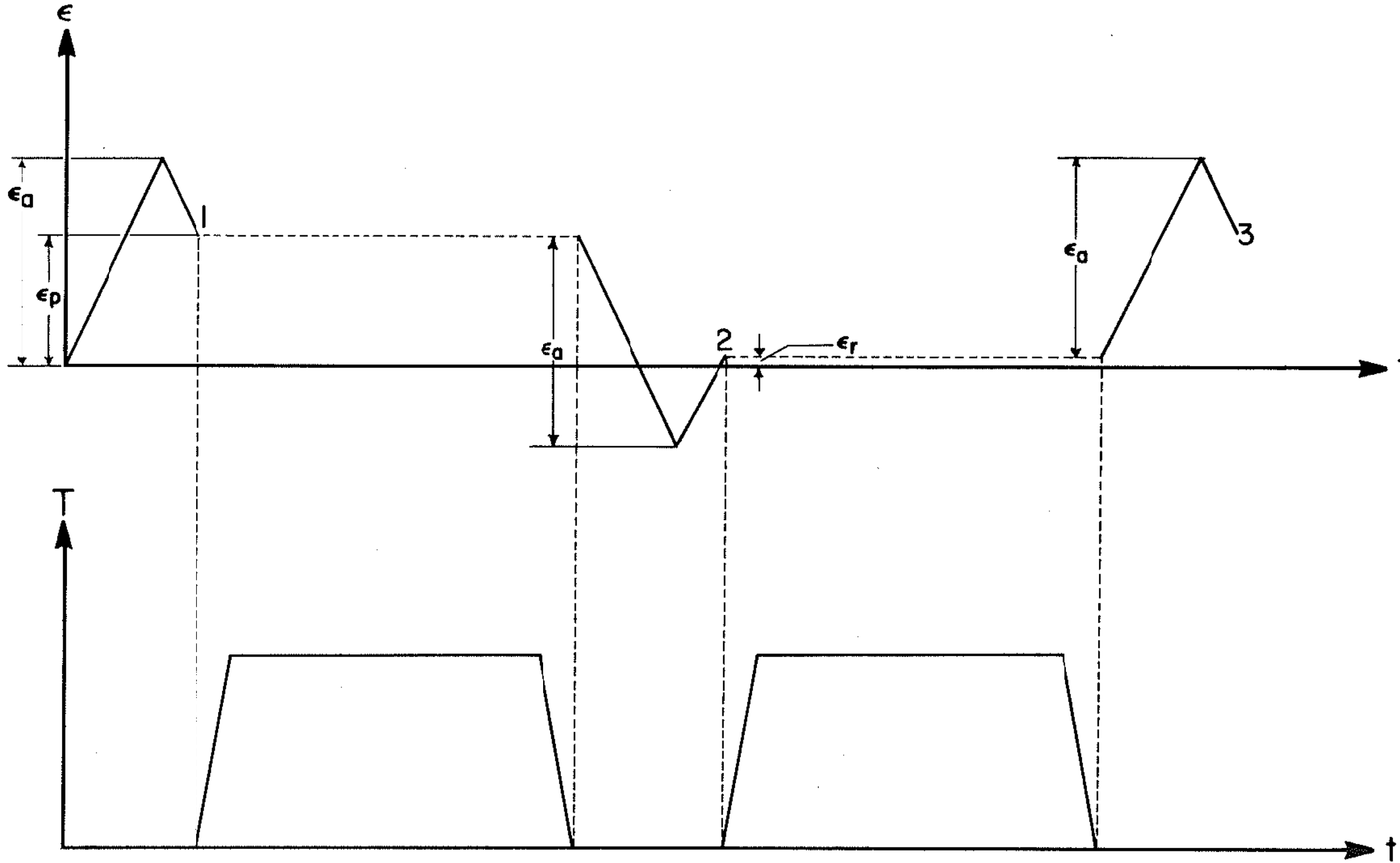


FIG. 4 APPLIED STRAIN AND TEMPERATURE AS A FUNCTION OF TIME

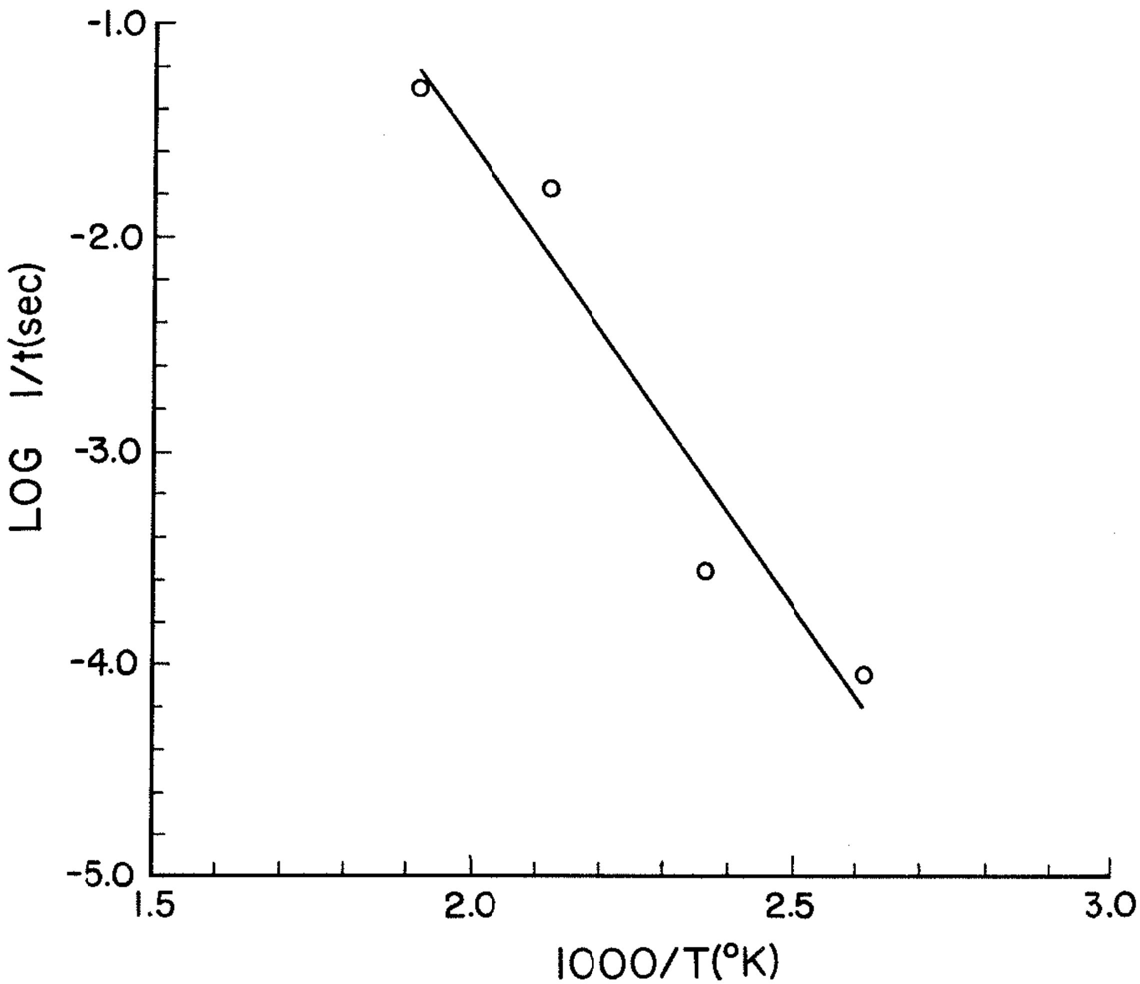


FIG. 5 AGING TIME-TEMPERATURE RELATIONSHIP FOR THE RECOVERY OF THE UPPER YIELD POINT

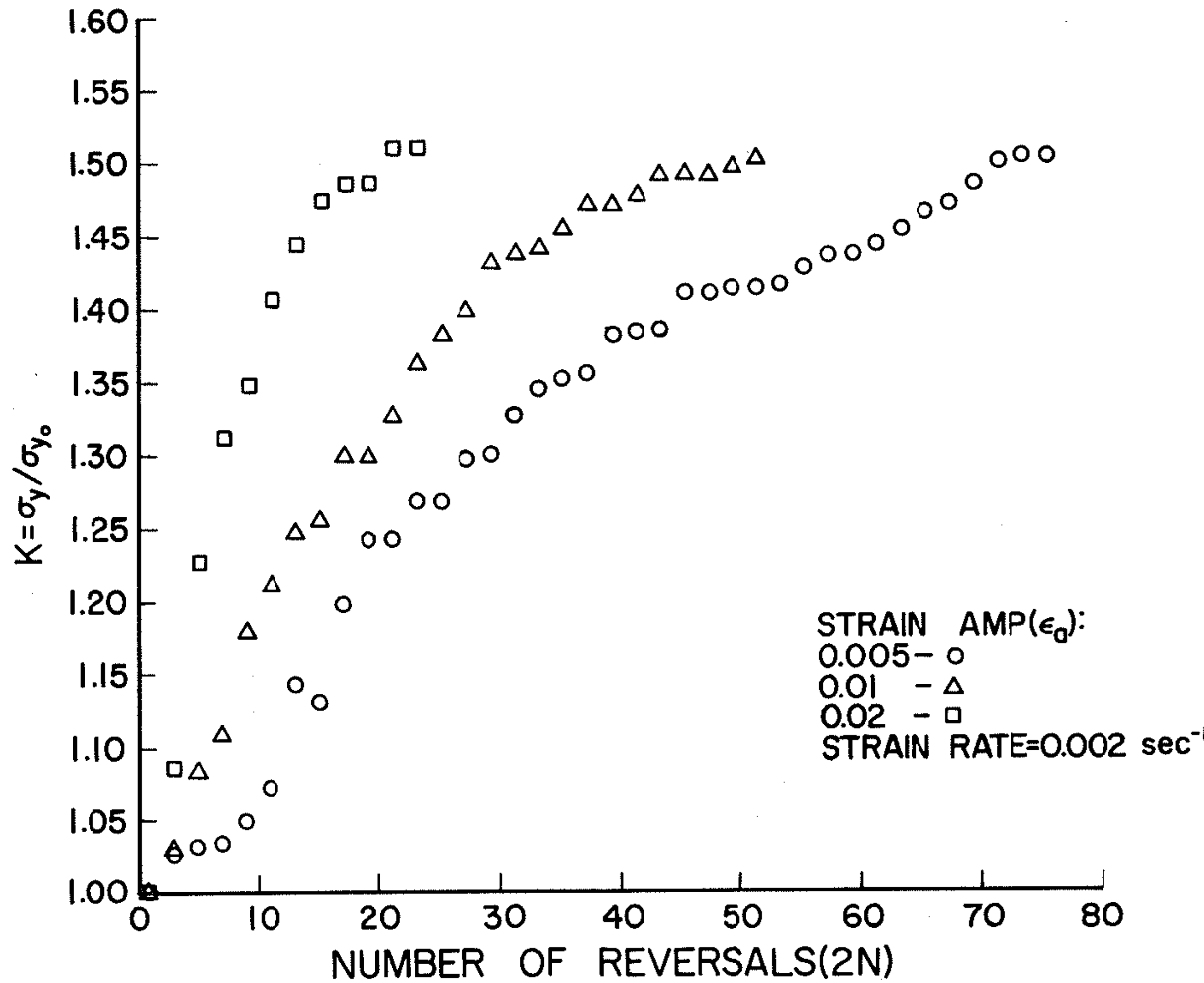


FIG. 6 TENSILE YIELD STRENGTH RATIO VERSUS NUMBER OF REVERSALS

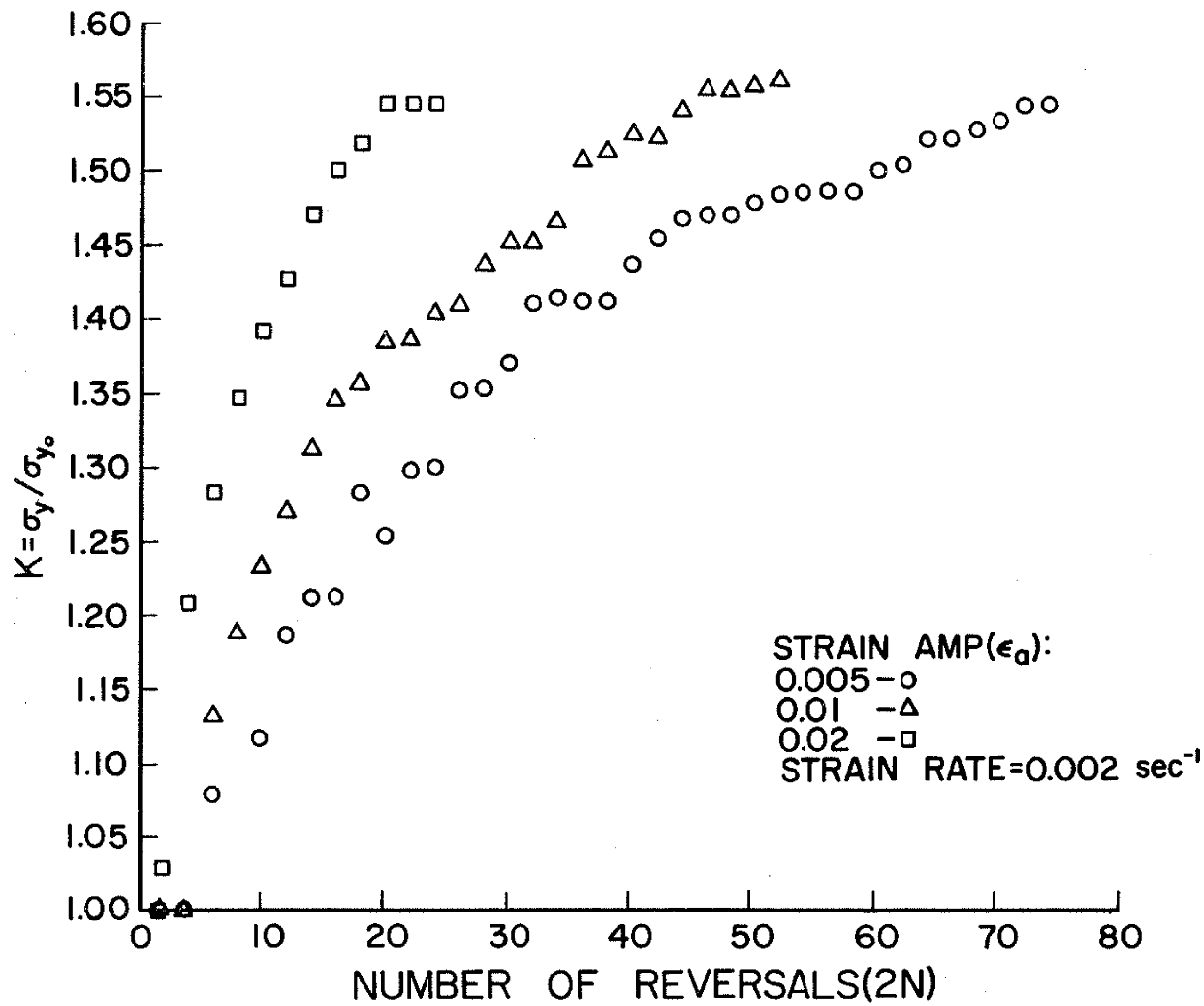


FIG. 7 COMPRESSIVE YIELD STRENGTH RATIO VERSUS NUMBER OF REVERSALS

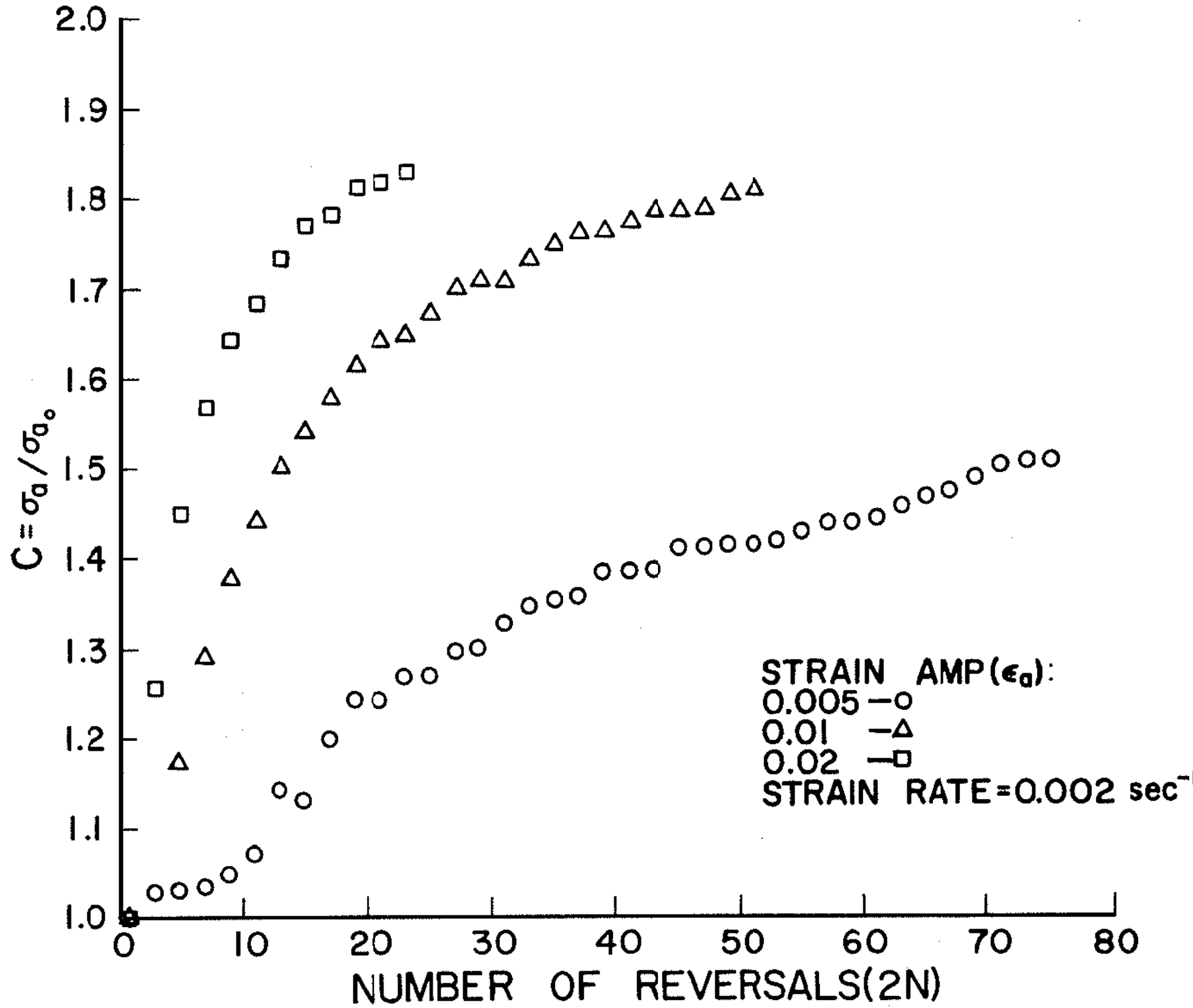


FIG. 8 TENSILE CYCLIC STRESS AMPLITUDE RATIO VERSUS NUMBER OF REVERSALS

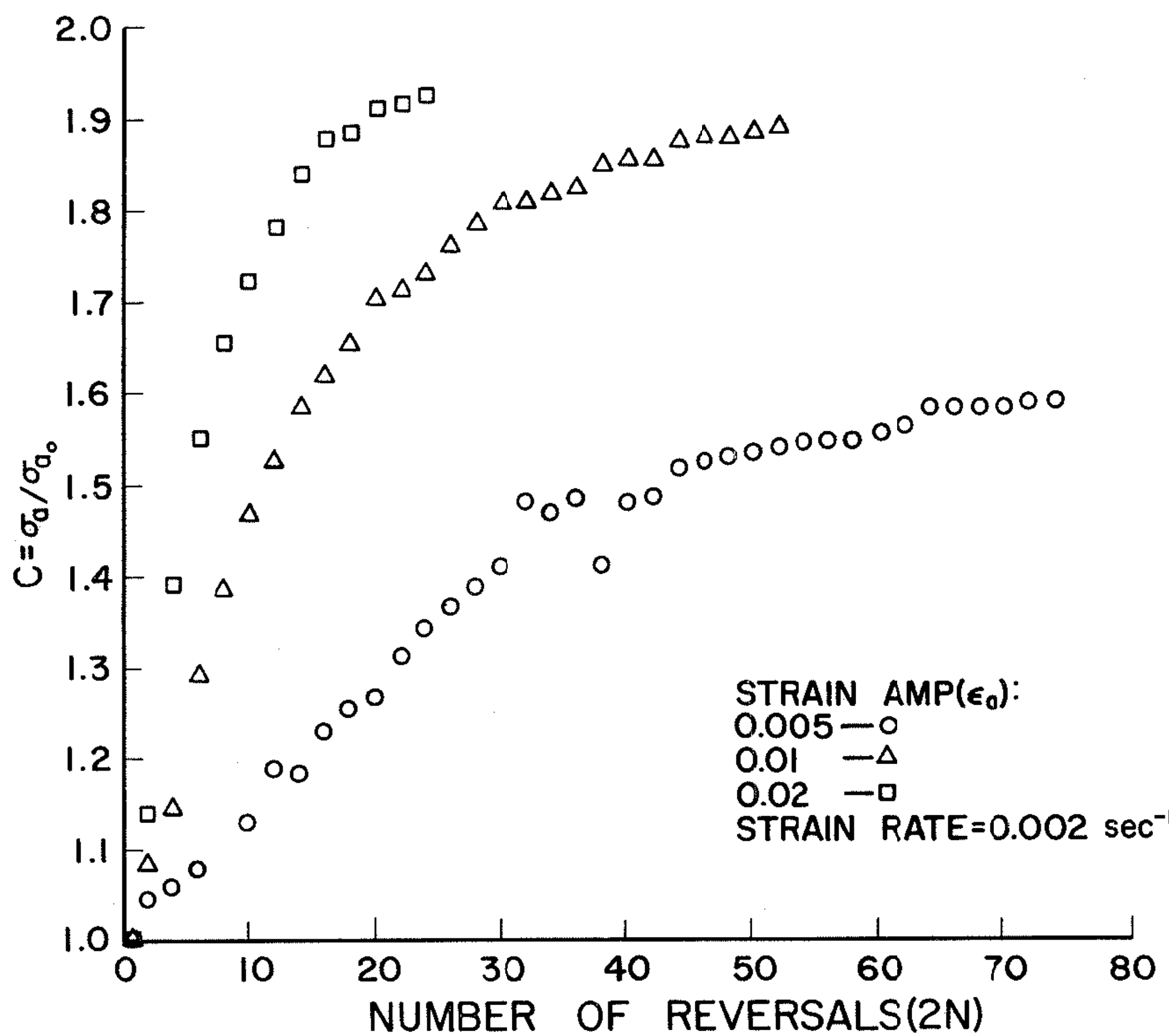


FIG. 9 COMPRESSIVE CYCLIC STRESS AMPLITUDE VERSUS NUMBER OF REVERSALS

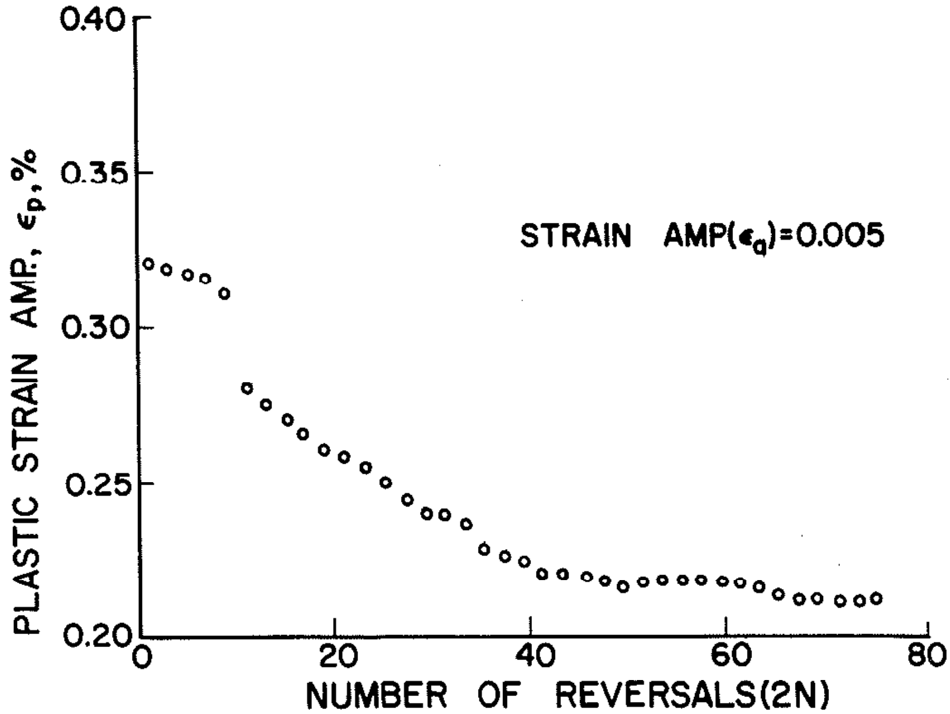


FIG. 10(a) PLASTIC STRAIN VERSUS NUMBER OF REVERSALS

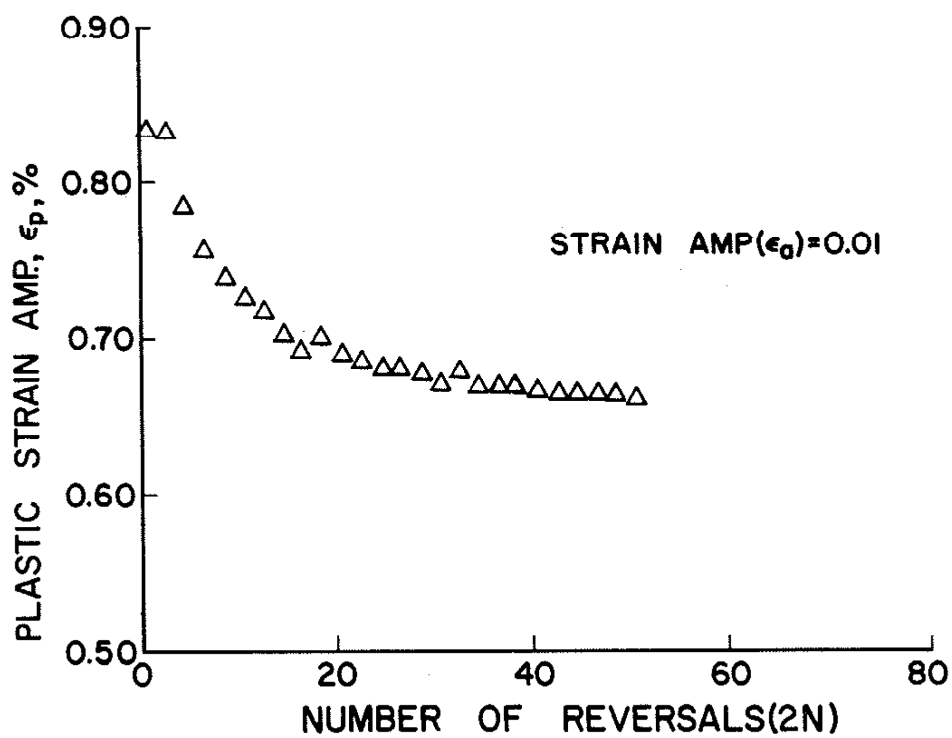


FIG. 10(b) PLASTIC STRAIN VERSUS NUMBER OF REVERSALS

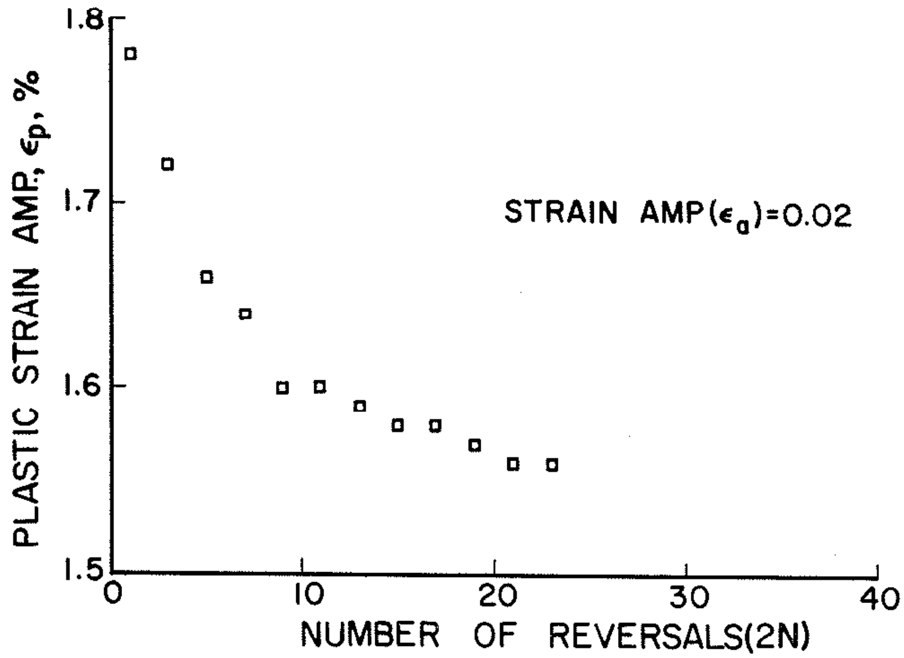


FIG. 10(c) PLASTIC STRAIN VERSUS NUMBER OF REVERSALS

STRAIN LIFE CURVE FOR ASTM A-36 (SINE WAVE)

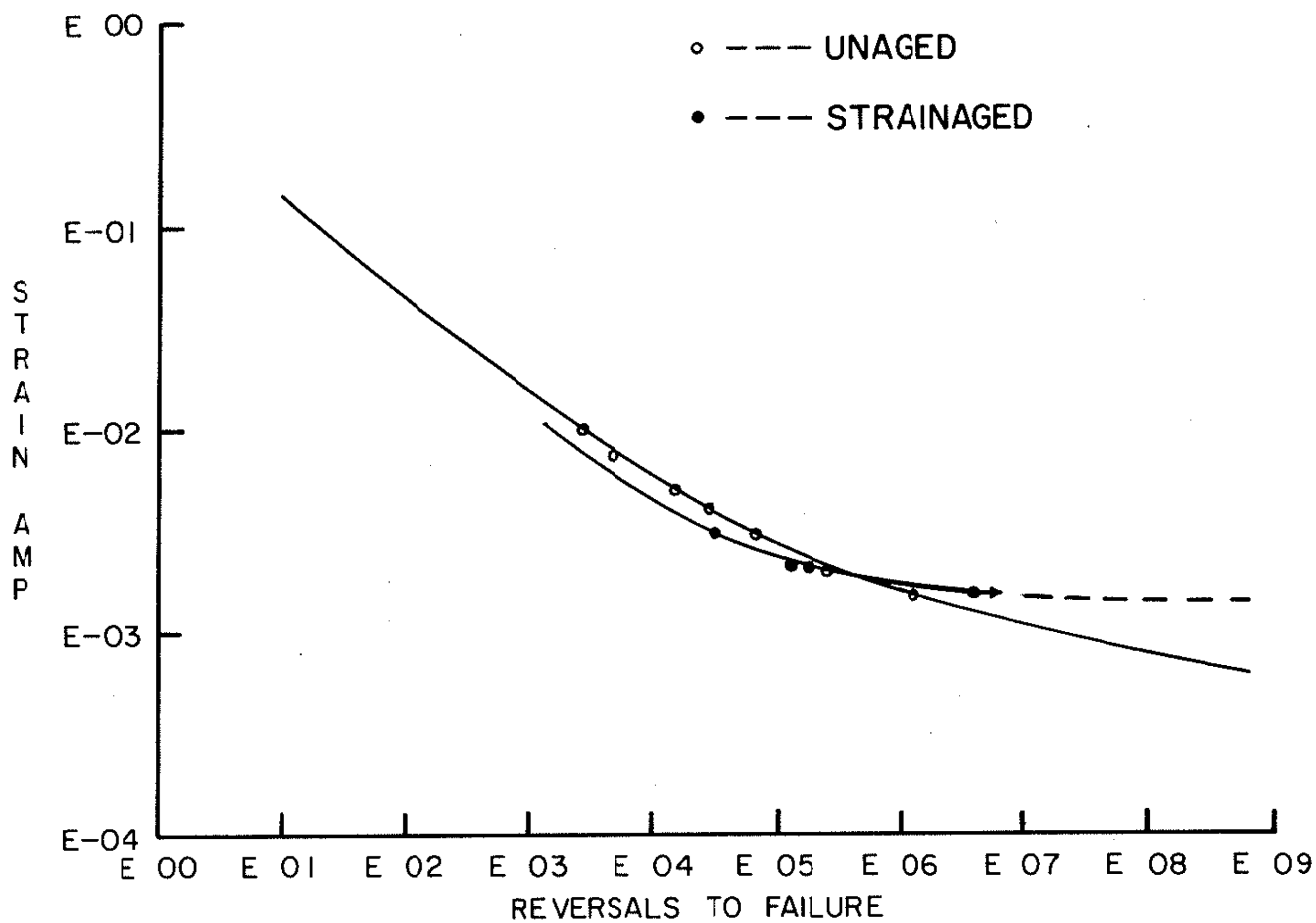


FIG. 11 STRAIN AMPLITUDE VERSUS NUMBER OF REVERSALS TO FAILURE

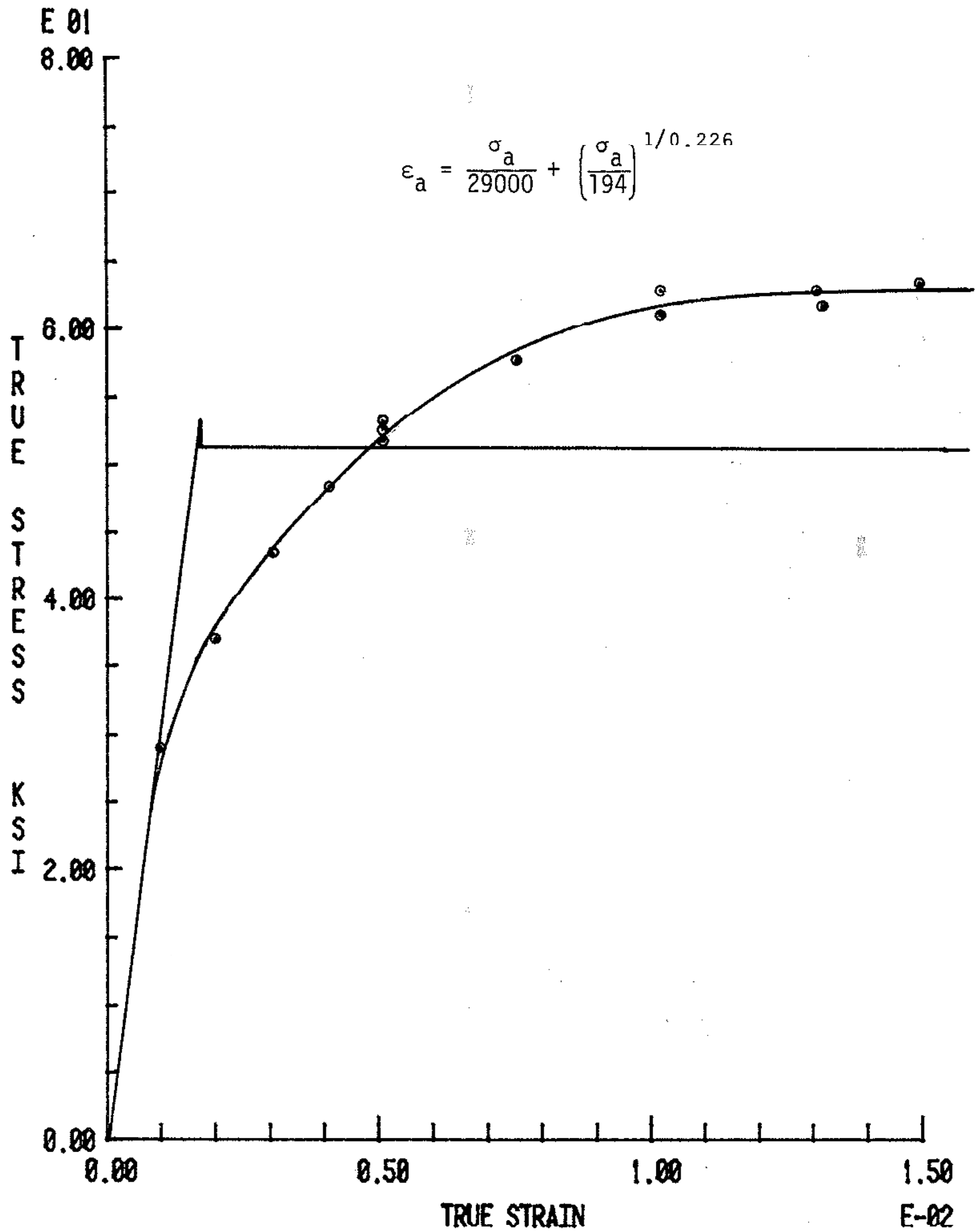


FIG. 12 MONOTONIC AND CYCLIC STRESS-STRAIN CURVE FOR ASTM A-36 (HOT ROLLED STRIP)

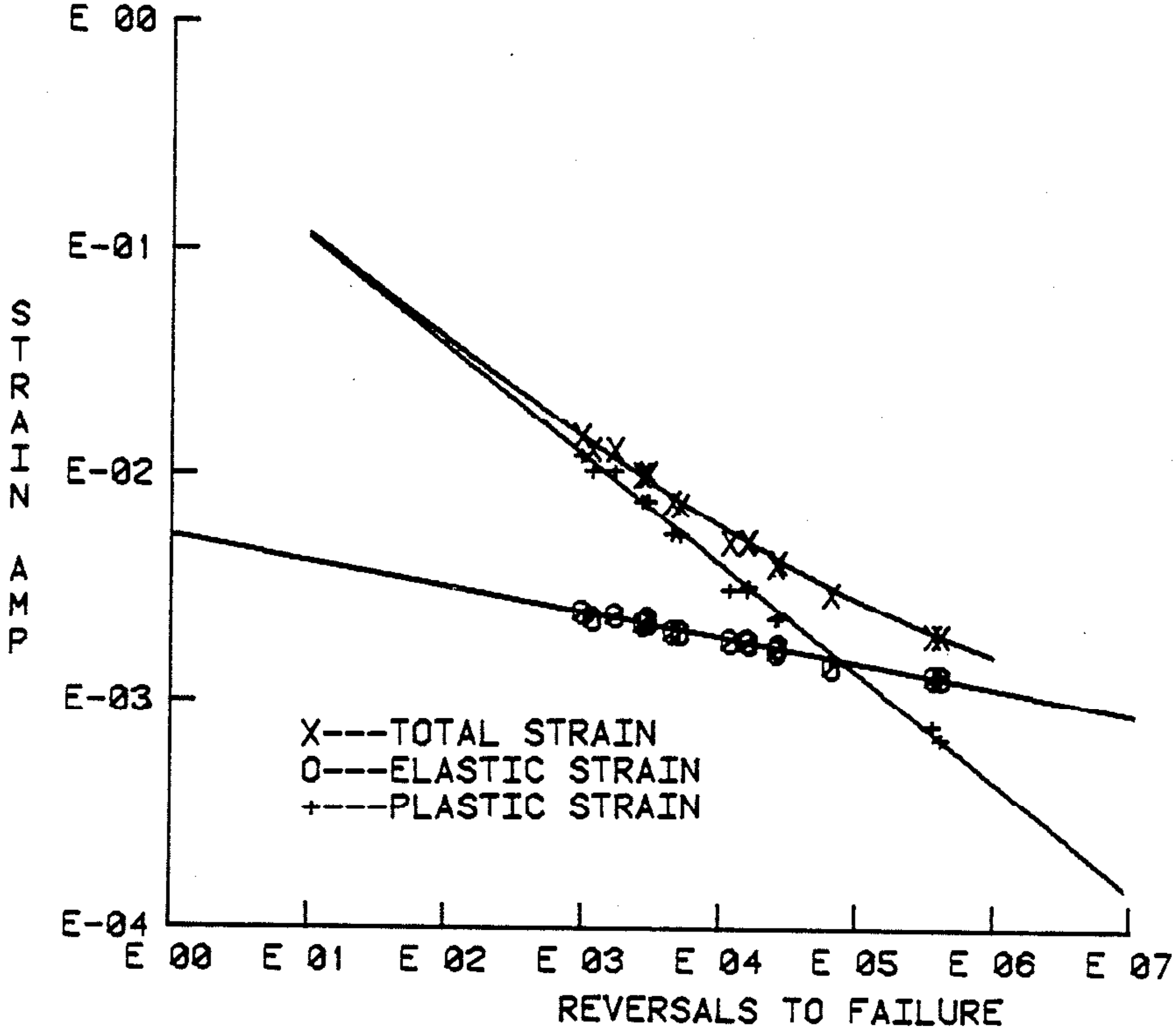


FIG. 13 STRAIN-LIFE CURVE FOR ASTM A-36 (HOT ROLLED STRIP)

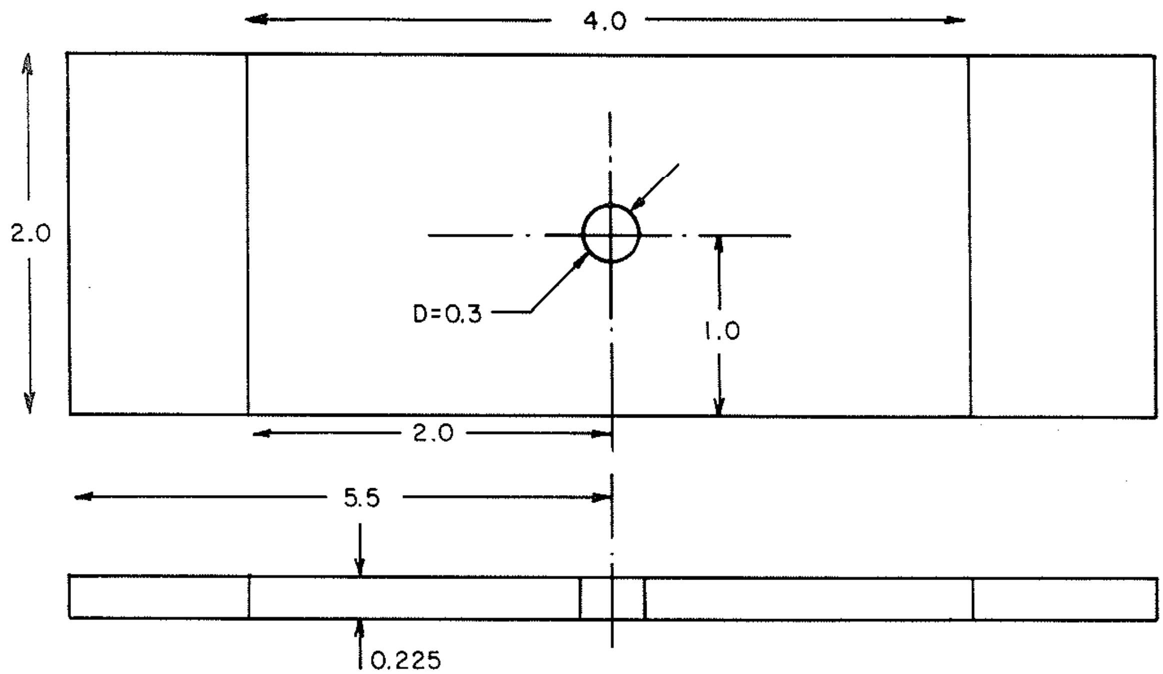


FIG. 14 CIRCULAR NOTCHED PLATE GEOMETRY

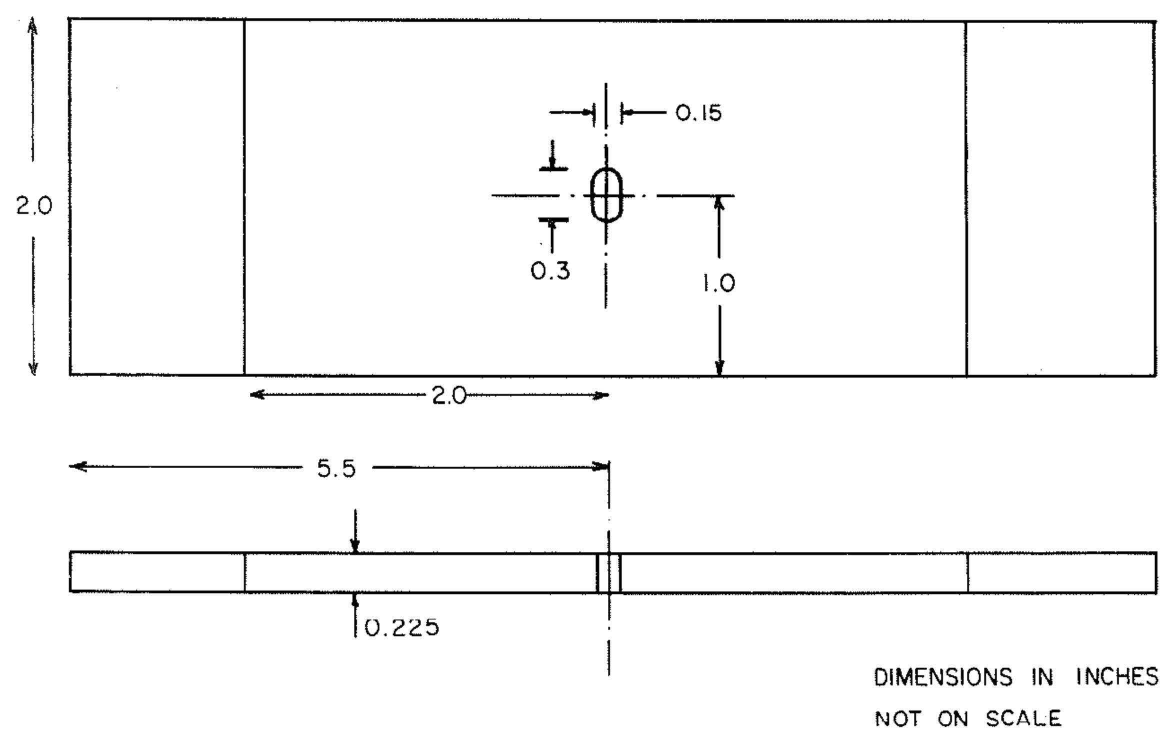


FIG. 15 SLOT NOTCHED PLATE GEOMETRY

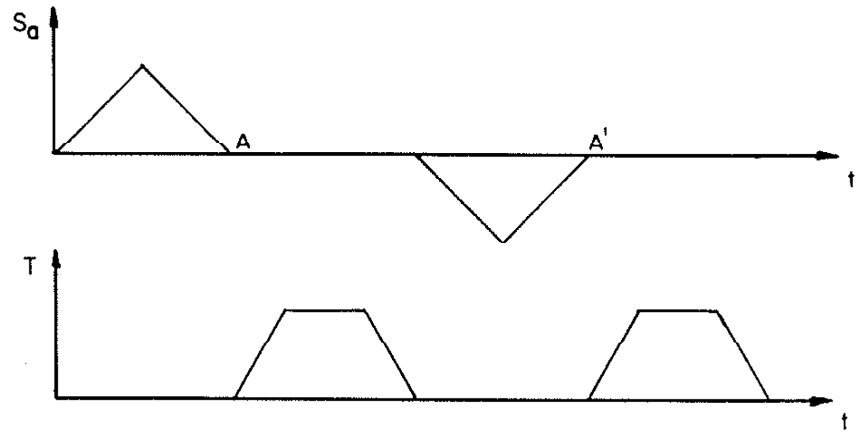


FIG. 16 REPEATED STRAIN AGING REVERSALS

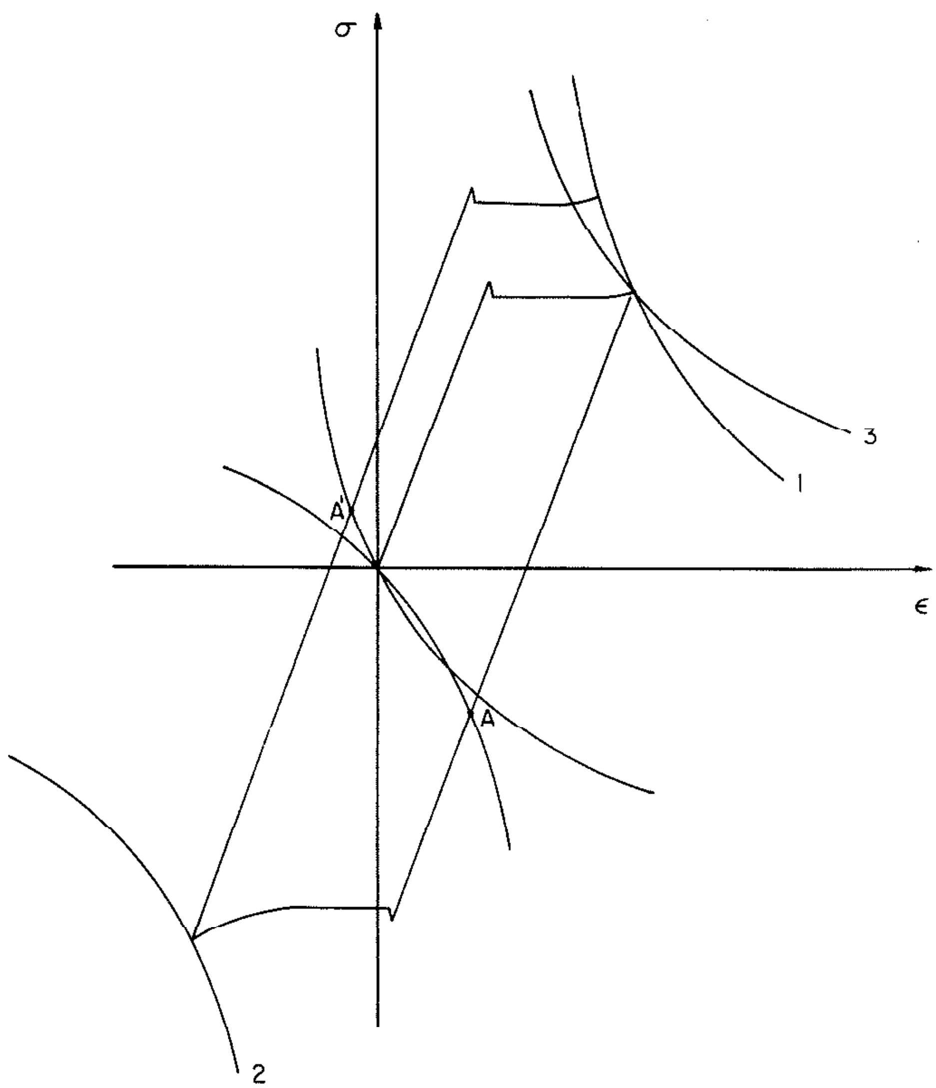


FIG. 17 STRESS-STRAIN RESPONSE AT THE NOTCH ROOT

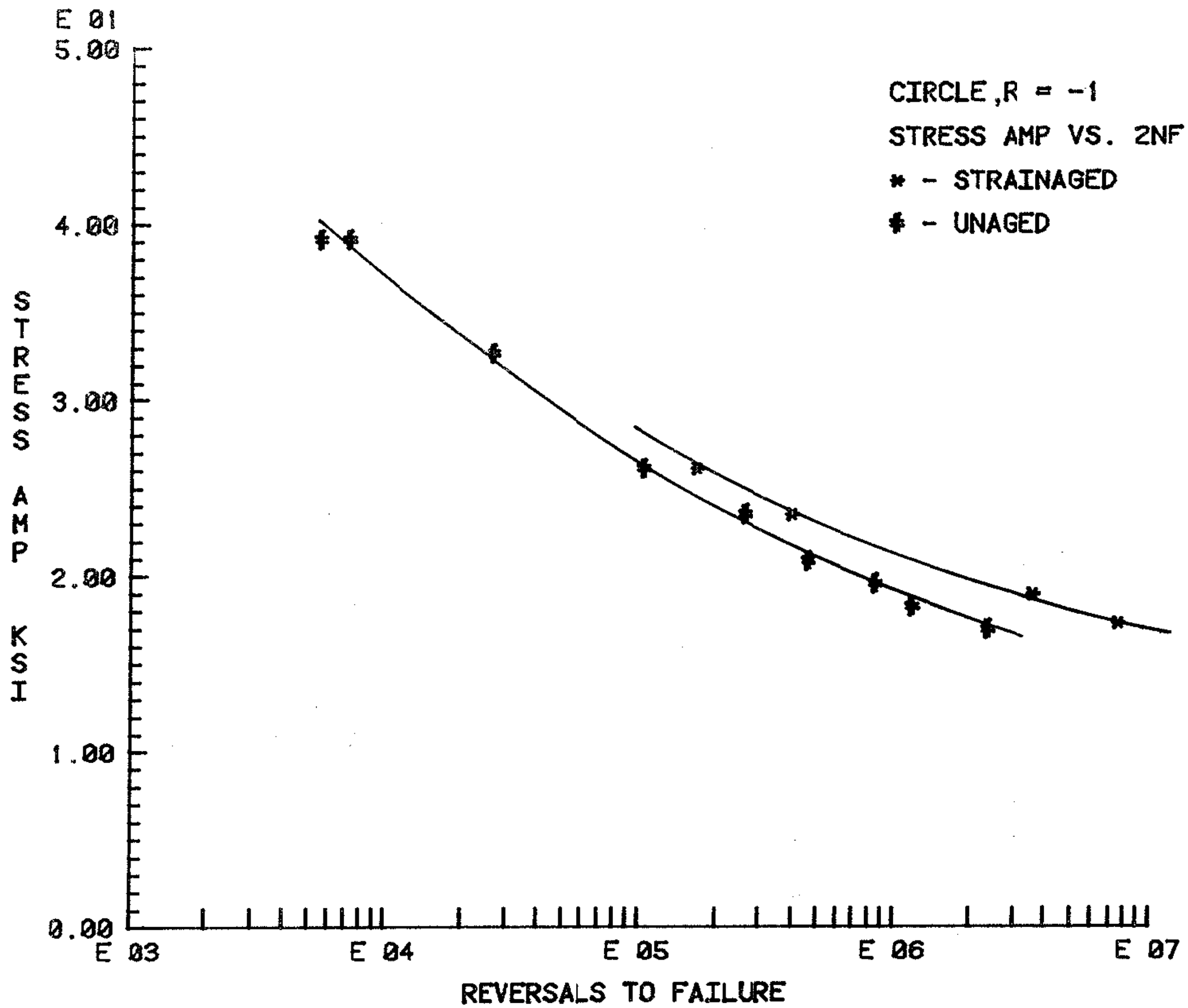


FIG. 18 STRESS AMPLITUDE VERSUS REVERSALS TO FAILURE FOR CIRCULAR NOTCHED PLATES

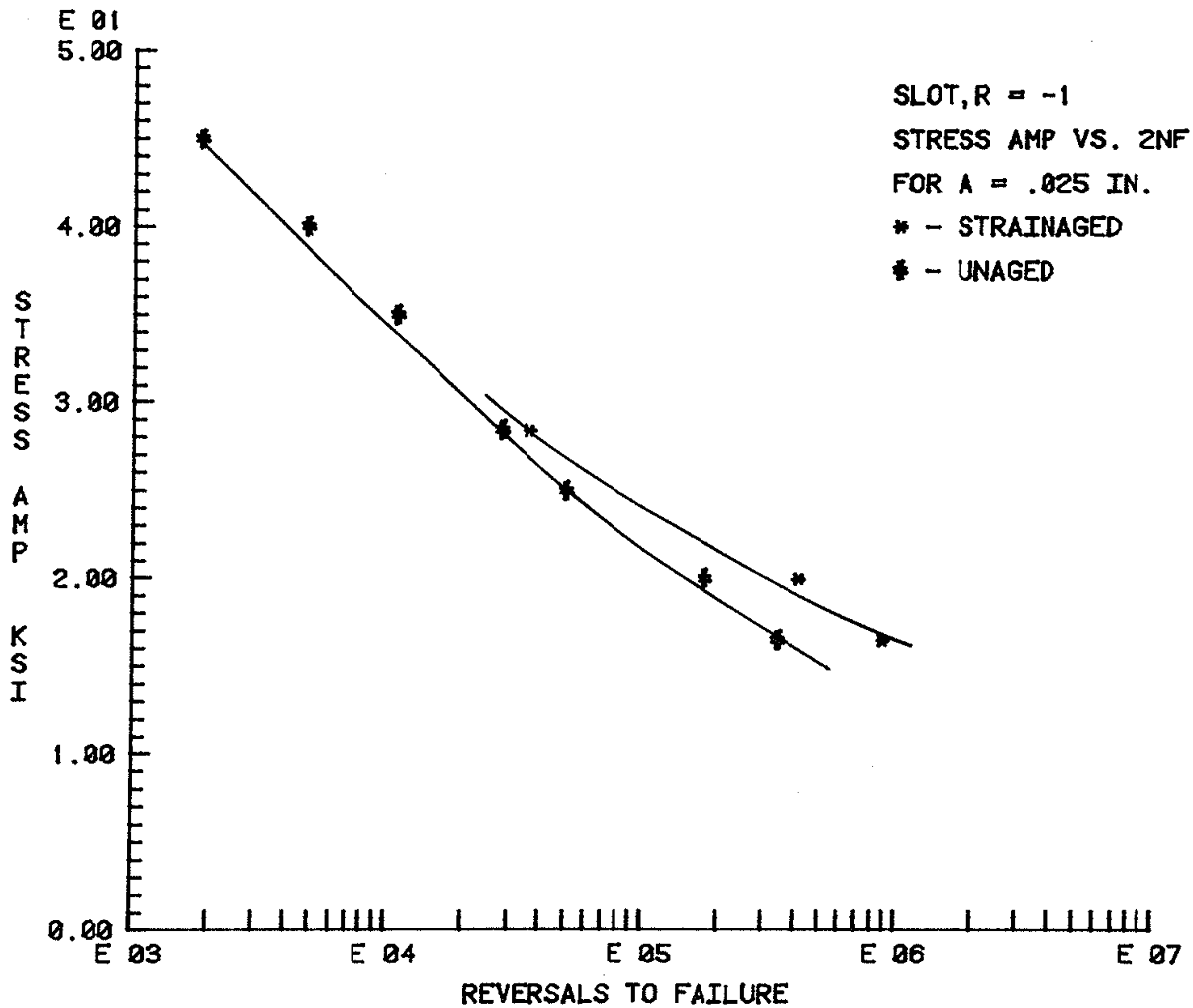


FIG. 19 STRESS AMPLITUDE VERSUS REVERSALS TO A CRACK LENGTH OF .025" FOR SLOT NOTCHED PLATES

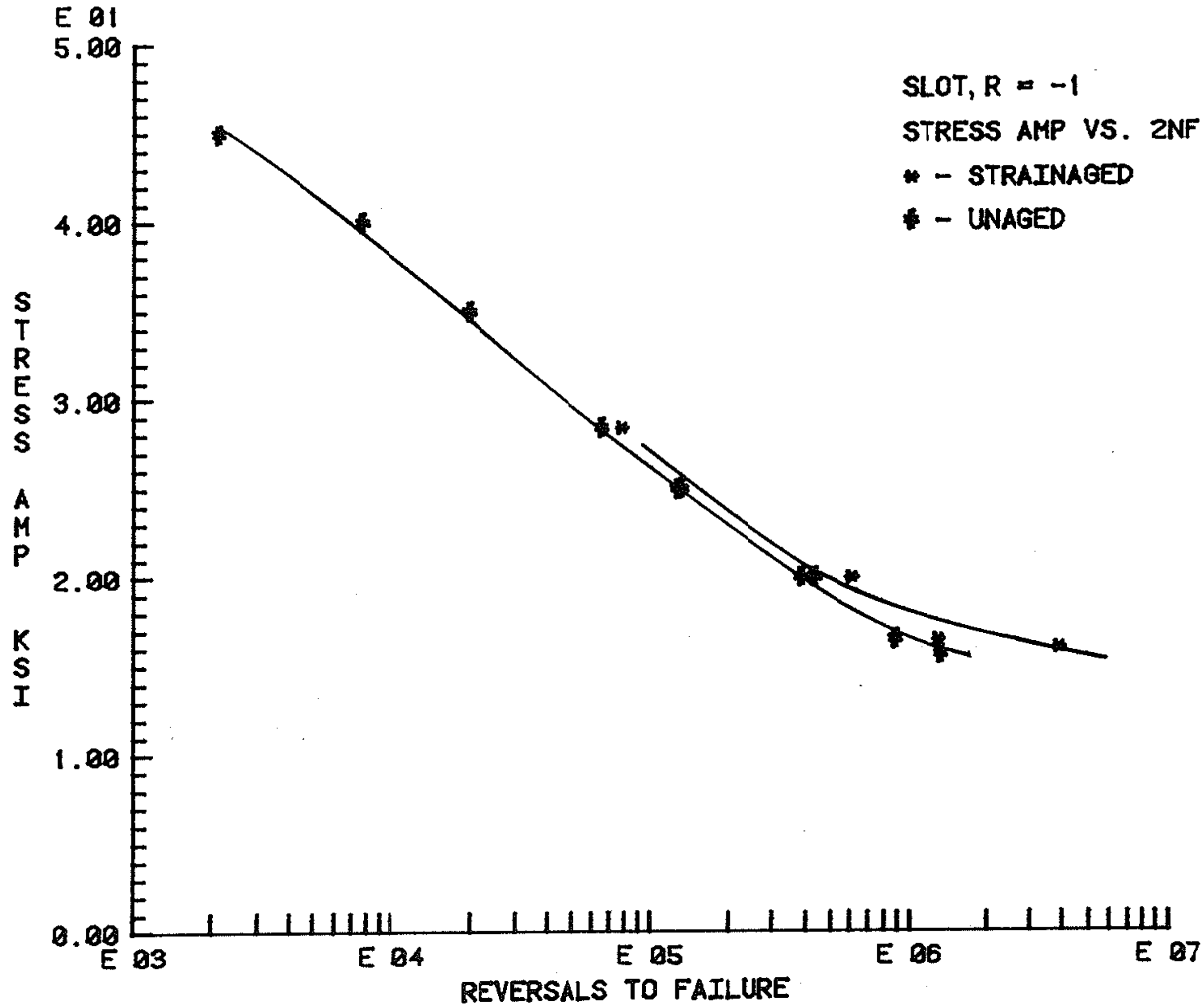


FIG. 20 STRESS AMPLITUDE VERSUS REVERSALS TO FAILURE FOR SLOT NOTCHED PLATES

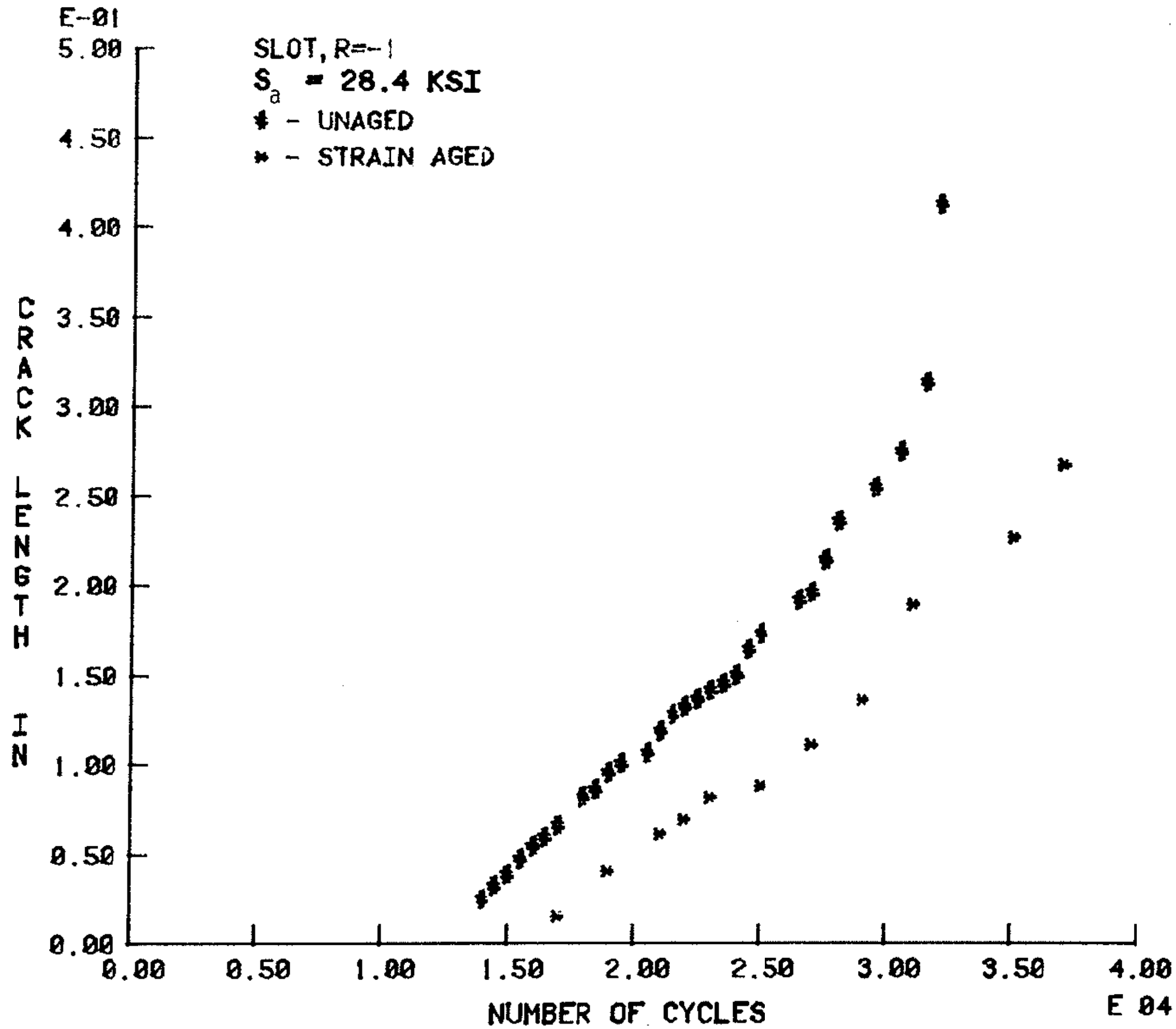


FIG. 21 CRACK LENGTH VERSUS NUMBER OF CYCLES FOR STRAIN AGED AND UNAGED SPECIMENS AT $S_a$ = 28 ksi (SLOT NOTCHED)

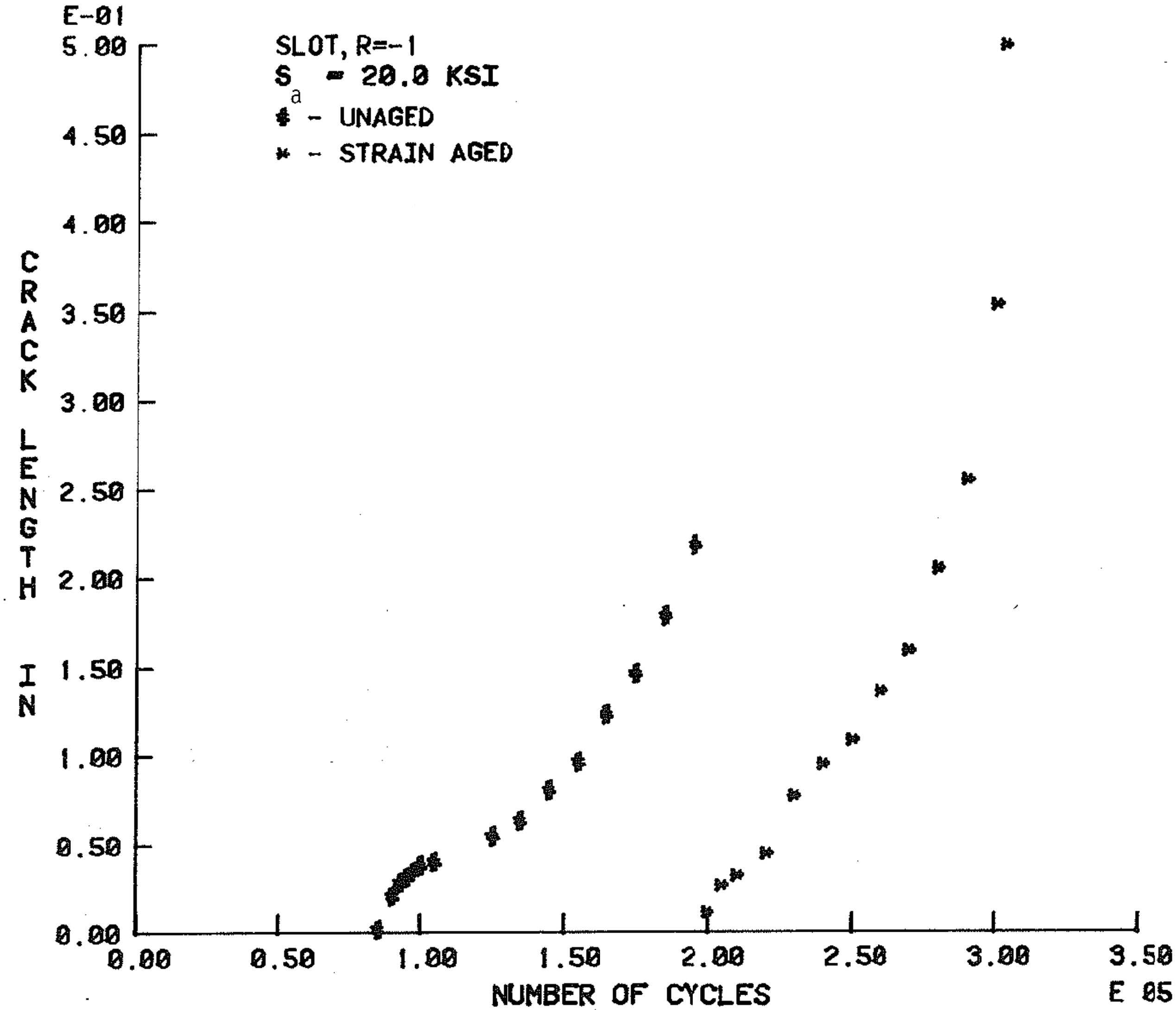


FIG. 22 CRACK LENGTH VERSUS NUMBER OF CYCLES FOR STRAIN AGED AND UNAGED SPECIMENS AT $S_a$ = 20 ksi (SLOT NOTCHED)

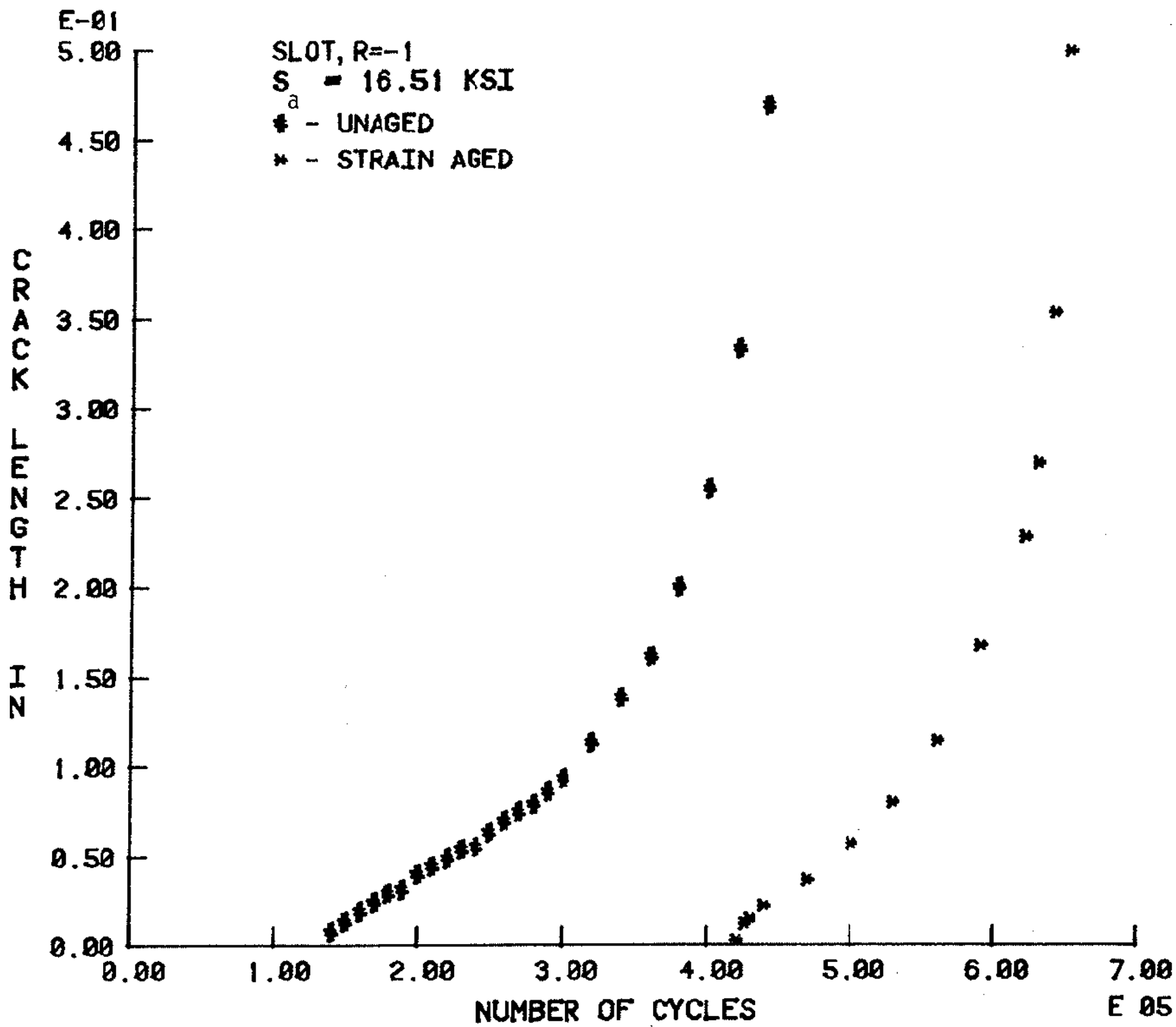


FIG. 23 CRACK LENGTH VERSUS NUMBER OF CYCLES FOR STRAIN AGED AND UNAGED SPECIMENS AT $S_a$ = 16.5 ksi (SLOT NOTCHED)

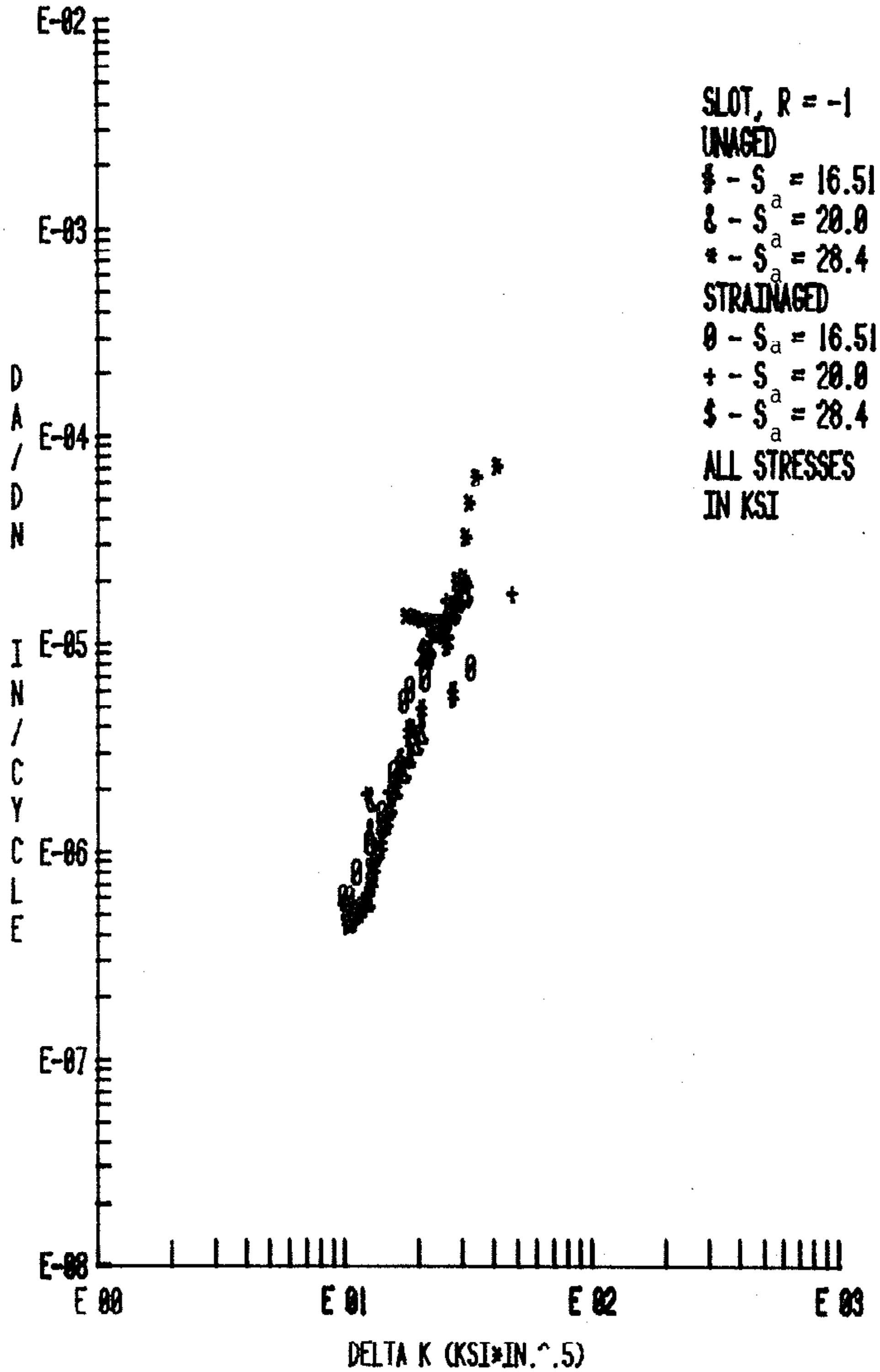


FIG. 24 da/dN VERSUS ΔK CHARACTERISTICS FOR STRAIN AGED AND UNAGED SLOT NOTCHED PLATES

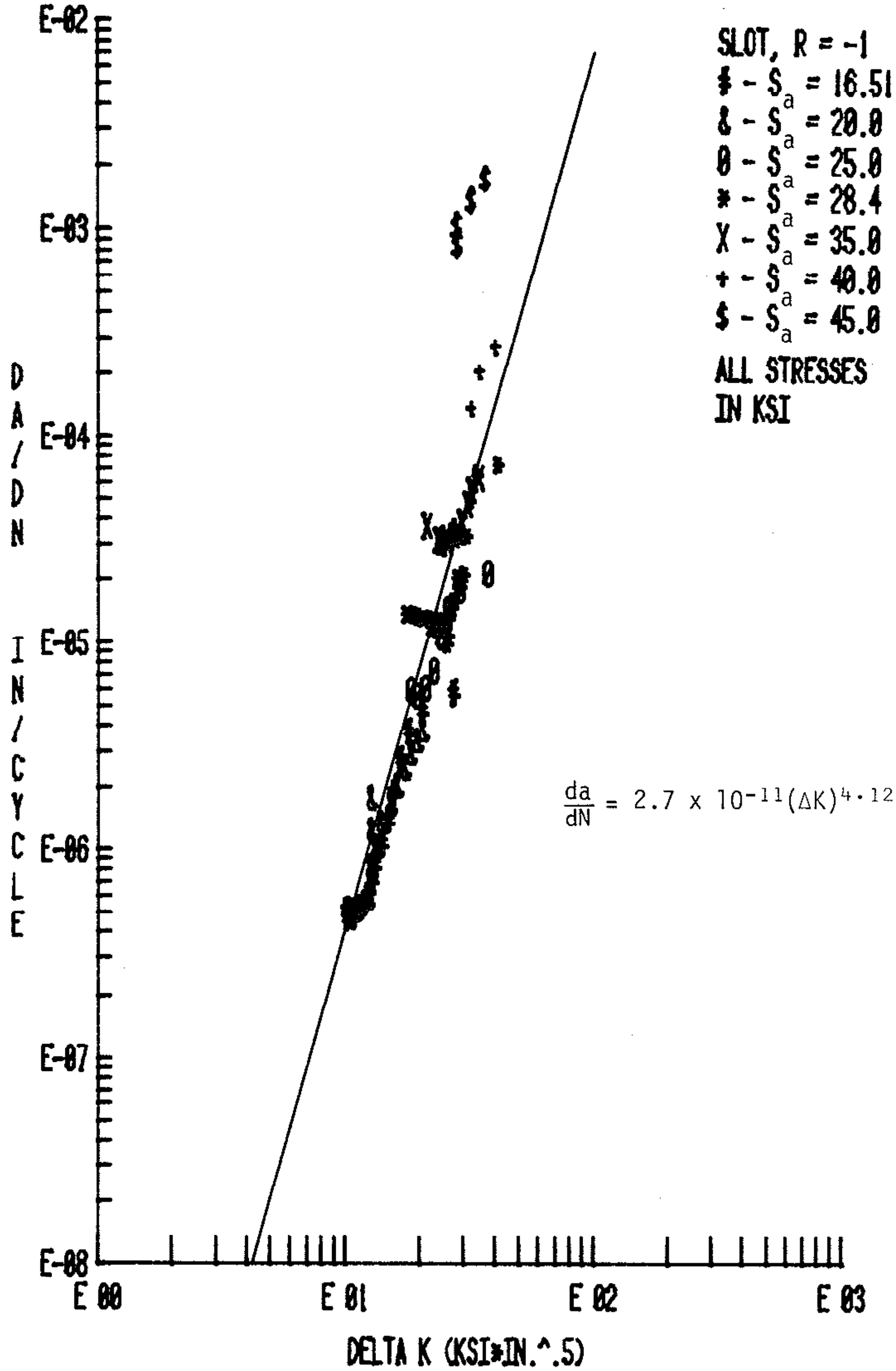


FIG. 25 da/dN VERSUS ΔK CHARACTERISTICS OF ASTM A-36 STEEL (R = -1)